INCORPORATING PHYSICAL OCEANOGRAPHIC PROXIES OF RECRUITMENT INTO POPULATION MODELS TO IMPROVE FISHERY AND MARINE PROTECTED AREA MANAGEMENT

J. WILSON WHITE
Dept. of Wildlife, Fish, and Conservation Biology
University of California, Davis
Bodega Marine Laboratory
PO Box 247
2099 Westside Road
Bodega Bay, CA 94923

present address:
Dept. Biology and Marine Biology
University of North Carolina, Wilmington
601 S. College Rd.
Wilmington, NC 28403
phone: 910-962-3058
fax: 910-962-4066
email: whitejw@uncw.edu

LAURA ROGERS-BENNETT
California Dept. of Fish and Game
Bodega Marine Laboratory
PO Box 247
2099 Westside Road
Bodega Bay, CA 94923

ABSTRACT

Variability in larval supply introduces uncertainty into the management of marine fisheries. This variability can confound short-term population projections of both traditional and spatially explicit models of fishery productivity. A potential remedy is the use of physical oceanographic variables, such as an upwelling index or the Pacific Decadal Oscillation, as proxies for recruitment year class strength. We describe a method for incorporating proxy information into population models for fishery management. Our model of a conventional fishery (using kelp rockfish as an example) suggested that proxies were effective in predicting actual larval survival if there was a strong correlation between the proxy and larval survival ($r > 0.8$), when recruitment was highly variable. Model outputs were most useful when used to hindcast rather than forecast the population trajectory. A spatial extension of the model for marine protected areas (MPAs) confirmed those results and revealed that 1) larval dispersal distances did not affect the utility of the proxy, and 2) adult home range size influenced whether before:after or inside:outside biomass ratios provided a more effective metric of MPA success. We found that proxies greatly improved model projections over short time scales, but that projections beyond the time needed for recruits to enter the fishery were less effective. This work provides an example of how information about environmental variability affecting recruitment can be incorporated into fishery models to improve management.

INTRODUCTION

A major difficulty encountered in the management of marine fisheries is the uncertainty introduced by variability in recruitment. It has been suspected for more than 100 years that physical factors affecting larval survival and transport drive much of this variability (Cushing 1982; Mullin 1994; Fogarty et al. 1991) and there have been attempts to find environmental variables which can predict recruitment success (Cushing 1982). Strong year classes (recruitment pulses or booms) can propagate through a fishery for multiple years and may sustain the fishery (Hjort 1914; Shepherd and Cushing 1990). The precise mechanism by which physical factors affect recruitment success is not always known and tends to be species-specific, but investigators have determined the nature of the link in a few cases (e.g., Gaines and Bertness 1993; Botsford et al. 1994; Peterson and Schwing 2003). More often, investigators report a relationship between recruit year-class strength and a physical proxy variable. Examples of such relationships have been reported for several fished species on the Pacific coast of North America. These include a correlation between recruitment of Dungeness crab (*Cancer magister*) and the Bakun upwelling index (Botsford and Wickham 1974), the timing of the spring transition (Shanks and Roegner 2007), and the Pacific Decadal Oscillation (Shanks et al. 2010). Likewise, settlement of kelp bass (*Paralabrax clathratus*) and nearshore rockfishes (*Sebastes* spp.) in southern California is related to a suite of oceanographic predictors over a range of spatial and temporal scales, including sea surface temperature, Ekman transport, and offshore wind stress (Caselle et al. 2010a). Total annual settlement of those nearshore rockfish species is strongly correlated with both the offshore and alongshore components of upwelling-associated transport (Caselle et al. 2010b). The information contained in these physical proxies may be useful in understanding recruitment variability and improving fisheries management.

Conceptually, a close relationship between a physical proxy and recruitment could be used to predict the short-term trajectory of recruitment, biomass, and yield when forecasting the possible consequences of different management options in a decision analysis context (Peterman and Anderson 1999; Harwood and Stokes 2003; Drechsler and Burgman 2004). Furthermore, a past record of year-class size could be used to distinguish signal (due to management) from noise (due to recruitment variability) in hindcasting models used to evaluate management actions in an adaptive management (sensu

Walters 1997) context. To our knowledge, no physical proxy has yet been incorporated into a population model used for adaptive management. Physical proxies however, are starting to be used as indicators of overall fisheries productivity. For example, an environmental parameter based on sea surface temperature is used to determine the harvest guideline for Pacific sardine, *Sardinops sagax* (Hill et al. 2007; but see McClatchie et al. 2010).

Management strategy evaluations, which simulate both population dynamics and management responses (Sainsbury et al. 2000), reveal the consequences of variable recruitment for stock assessment and the adaptive management of fishery stocks. The management problem is that realistic levels of process error (sensu Hilborn and Mangel 1997) in annual recruitment can cause projected biomass to vary over several orders of magnitude among simulations with the same deterministic dynamics. Examples of this problem have been shown for the adaptive management of many species, including rockfishes (*Sebastes* spp.) from the U.S. Pacific coast (Punt and Ralston 2007), Gulf of Alaska walleye pollock (*Theragra chalcogramma*; A'mar et al. 2008) and several key fishery species in southeast Australia (Punt et al. 2000). Although the minimum value of spawning potential ratio (SPR) (expected lifetime egg production) needed for population persistence is uncertain and depends on larval processes, the SPR itself is not sensitive to interannual variations in recruitment (Hilborn et al. 2002). However, the management status of a stock is typically estimated in terms of biomass or catch (e.g., Ralston 2002; Rose and Cowan 2003; Punt and Ralston 2007), which are highly sensitive to physically-forced variability. Additional uncertainty is introduced when there is a time lag between spawning and recruitment. This introduces a lag between the implementation of a new management action and its effects on the fishery, and can lead to management that tracks noise rather than the deterministic signal (Punt and Ralston 2007).

The problems of recruitment variability are compounded in the management of marine protected areas (MPAs), which adds the spatial dimension. Management of MPAs ideally involves monitoring populations inside MPAs using a Before-After Control-Impact (BACI) design so that the deterministic effects of MPAs on fished populations can be distinguished from large-scale, environmental forcing across areas (Underwood 1994; Fraschetti et al. 2002; Grafton and Kompas 2005; Russ et al. 2008). However, monitoring may not start at the time of implementation (Fraschetti et al. 2002) and as a consequence it is common to measure trajectories of a response variable (e.g., biomass) inside and outside MPAs to quantify differences between fished regions and MPAs (e.g., Hamilton et al. 2010). However, the effectiveness of this approach is likely to be sensitive to 1) movement of adults and larvae between fished and unfished regions, 2) the intensity of fishing outside MPA boundaries, 3) the lag time between MPA implementation and recruitment, and 4) the strength of the signal:noise ratio introduced by recruitment variability. The first two factors make it difficult to measure the effects of MPAs over both long and short time scales (Botsford et al. 2001; Moffitt et al. 2009; White et al. 2010b); while factors 3 and 4 hold for both nonspatial and spatial management over the short term only. Here we focus primarily on the problems introduced by lag times and signal:noise ratios related to recruitment variability as the first two topics have been considered in detail elsewhere (Moffitt 2009; Moffitt et al. 2009; White et al. 2010b).

Here we develop a method for incorporating physical proxies of larval production into population models used for fishery management and assessment. We first develop a model of a conventionally managed fishery, then extend the model to include spatial management. In both cases we first illustrate the use of prospective modeling (forecasting), for decision analysis at the time of an initial management action. We then consider the use of retrospective modeling (hindcasting), in which we simulate the trajectory between an initial decision and a later observation. In this modeling work we use kelp rockfish, *Sebastes atrovirens,* as an example of a typical nearshore fished species for which physical proxies for recruit year-class strength exist (Caselle et al. 2010b). The goal of this modeling work is to determine if the addition of the physical proxy aids in distinguishing deterministic changes in recruitment from stochastic variability in order to evaluate its potential for guiding management decisions and implementing adaptive management.

METHODS

We implemented a discrete time, spatially explicit, age-structured, single-species model of a typical rocky reef species. We incorporated von Bertalanffy growth, a nonlinear length-weight relationship, and fecundity proportional to biomass. Adults spawn pelagic larvae during an annual reproductive period, larvae disperse according to a dispersal matrix, and settling larvae experience density-dependent survival following a Beverton-Holt survivorship function. The model follows the basic structure used by White et al. 2010b and can be summarized by the following equations, taking $\mathbf{N}_j(t)$ to be the vector of abundances of each of A age classes in spatial cell j (out of n total cells) at time t (Table 1 summarizes symbols used in this paper; boldface symbols indicate vectors and matrices). The number of larval settlers arriving at cell i, S_i, is

$$S_i(t) = \sum_{i=1}^{n} D_{ij} f\left(\mathbf{N}_j(t)\right) \frac{1}{1+e^{-\theta(t)}} \qquad (1)$$

TABLE 1
Symbols used in the paper

Symbol	Sub-element	Definition
State variables		
$\mathbf{N}(t)$	$\mathbf{N}_i(t)$	Abundance of each age classes in each cell at time t ($A\times n$ matrix)
$\mathbf{N}_i(t)$	$N_{i,a}(t)$	Abundance of each age class in cell i at time t ($A\times 1$ vector)
$S_i(t)$		Number of settlers in cell i at time t
SSB(t)	$SSB_i(t)$	Spawning stock biomass in cell i at time t ($n\times 1$ vector)
Parameters		
α		Density-independent Beverton-Holt settler survival
a_0		Age at size 0
a_c		Age at recruitment into fishery
a_m		Mean age at maturity
β		Asymptotic Beverton-Holt maximum recruit density
b		Fecundity per unit biomass
γ		Length-biomass exponent
$\mathbf{D}$	D_{ij}	Probability of larval disperal from cell j to cell i
$F_i(a)$		Fishing mortality rate for age a individuals in cell i
$\widehat{F}_i(a)$		Effective fishing rate experienced due to home range movement
F_{MSY}		Value of F that produces maximum sustainable yield
h		Radius of adult homerange
k		von Bertalanffy growth rate
L_∞		von Bertalanffy Asymptotic maximum length
M		Natural mortality rate
q		Length-biomass coefficient
ρ		Correlation between $\boldsymbol{\theta}$ and $\boldsymbol{\phi}$
Other		
A		Number of age classes
$B(a)$		Biomass at age a
CRT		Critical replacement threshold
cv_θ		Coefficient of variation of $\theta(t)$
$f(\mathbf{N}_i(t))$		Fecundity at cell
$\lambda_{\mathbf{D}}$		Leading eigenvalue of $\mathbf{D}$
$L(a)$		Length at age a
LEP		Lifetime egg production
LEP_{pre}		Fraction of lifetime egg production (relative to unfished maximum) at $t \le 0$
LEP_{post}		Fraction of lifetime egg production at $t > 0$
n		Number of spatial cells
$\boldsymbol{\phi}$	$\phi(t)$	Physical factor affecting larval survival
$p(a)$		Probability of maturity at age a
s_θ		standard deviation of $\theta(t)$
s_ϕ		standard deviation of $\phi(t)$
SPR		spawning potential ratio
$\boldsymbol{\theta}$	$\theta(t)$	Larval survival parameter
$\widehat{\boldsymbol{\theta}}$		Values of $\boldsymbol{\theta}$ predicted from a particular $\boldsymbol{\phi}$ without accounting for ρ
X'		Simulated value of variable X, incorporating process variability
X*		Actual value of variable X corresponding to simulated value X'

where D_{ij} is the i,j^{th} element of the dispersal matrix $\mathbf{D}$ and gives the probability of larvae dispersing from j to i. The term including $e^{-\theta(t)}$ represents larval survival and is explained below. The scalar $f(\mathbf{N}_j)$ is the total fecundity of the population at j:

$$f\left(\mathbf{N}_j(t)\right) = SSB_j(t)b \tag{2a}$$

$$SSB_j(t) = [p(1)B(1), p(2)B(2), \ldots p(3)B(A)] \times \mathbf{N}_j(t) \tag{2b}$$

where $\times$ represents vector multiplication, $SSB_j(t)$ is spawning stock biomass, b is fecundity per unit biomass, $p(a)$ is the probability of being reproductively mature at age a (assumed to be 0 for $a < a_m$ and 1 for $a \ge a_m$), and $B(a)$ is mean biomass at age a. Biomass is a function of length, $B(a) = qL(a)^r$, where q and r are constants. Length at age is given by a von Bertalanffy function with growth rate k, age at length zero a_0, and asymptotic maximum length L_∞:

$$L(a) = L_\infty \left[1 - e^{-k(a-a_0)}\right] \tag{3}$$

Note that for simplicity we assume there is no variability in length or biomass at age.

The updating step for the population is given by Equation 4 (see Equation 4, next page).

Note that the initial age class in $\mathbf{N}_j(t+1)$ is comprised of settlers $S_j(t)$ that survive Beverton-Holt density-dependent mortality (with density-independent survivorship α and asymptotic maximum settler density β). Post-settlement individuals have density-independent mortality rate M and experience fishing rate $F(a)$, which is a function of age such that $F(a) = 0$ for all $a < a_c$, the age at which individuals recruit to the fishery; $F(a)$ is constant for all $a \ge a_c$ and was varied to create different fishing scenarios (fishery mortality typically depends on length not age; because our model has deterministic growth, length and age are directly related by Equation 3, so age a_c corresponds to a particular length). Demographic parameter values were taken from literature estimates for kelp rockfish, *Sebastes atrovirens* (tab. 2). In all cases we assume data are fisheries-dependent, so direct observation of age classes younger than a_c is impossible.

The major difference in model structure from typical models of this type (e.g, White et al. 2010b) is that we explicitly modeled larval survival. Following the convention used in statistical survival analysis, we assumed that larval survival was a logit function of parameter $\theta(t)$, so that larval survivorship is equal to $\text{logit}^{-1}(\theta(t)) = 1/(1+\exp(-\theta(t)))$. This relationship allows $\theta(t)$ to vary widely but constrains survival to fall between 0 and 1; alternative functional forms could be substituted as appropriate for a specific study system. We assumed that $\theta(t)$ is a function of some physical oceanographic factor, and is correlated, with correlation coefficient ρ, to

$$\mathbf{N}_j(t+1) = \begin{bmatrix} 0 & & & & \\ e^{-(M+F(1))} & & & & \\ & e^{-(M+F(2))} & & & \\ & & \ddots & & \\ & & & e^{-(M+F(A-1))} & 0 \end{bmatrix} \times \mathbf{N}_j(t) + \begin{bmatrix} \dfrac{\alpha S_j(t)}{1+\dfrac{\alpha}{\beta}S_j(t)} \\ 0 \\ \vdots \\ 0 \end{bmatrix} \quad (4)$$

TABLE 2
Life history parameters for kelp rockfish, *Sebastes atrovirens*, used in the model

Parameter	Estimate	Notes
Beverton-Holt settler survival $R = \alpha S/(1+(\alpha/\beta)S)$		
α	4.86	a
β	1	b
Length-at-age (cm) $L(a) = L_\infty\,(1-\exp(-k(a-a_0)))$		
L_∞	37.8 cm	c
k	0.23 y^{-1}	
a_0	–0.7 y	
Weight-at-length (kg) $W = pL^q$		c
p	9.37×10^{-6} kg cm^{-q}	
q	3.172	
A	25 y	d
a_m	4 y	d
M	0.2 y^{-1}	e
a_c	4 y (29 cm)	f
$\bar{\theta}$	0.5	g

Notes:
a. Fitted to produce CRT = 0.25, given other demographic parameters
b. Arbitrary; this parameter defines spatial scale at which density is calculated but does not affect model results
c. Source: Lea et al. (1999)
d. Source: Love et al. (2002)
e. Not well known; value based on lifespan given in Love et al. (2002)
f. Based on California Department of Fish and Game regulations
g. Arbitrary; because a is scaled to produce a given CRT, model results are not sensitive to this value

some observable quantity $\phi(t)$, e.g., sea surface temperature, an upwelling index, the timing of a seasonal current shift, Pacific Decadal Oscillation, etc. For example, in kelp rockfish, Caselle et al. (this issue) have documented correlations between larval settlement (a function of larval survival) and the strength of the offshore component of upwelling transport with values of r as high as 0.99. For the purposes of the model, we assume that $\phi(t)$ is some generic quantity that is recorded annually. Thus, given past observations of $\phi(t)$, it is possible to re-create the pattern of $\theta(t)$ (with precision determined by ρ) and thus approximate the pattern of larval survival, even when observations of the resulting age classes are not yet available.

The persistence of an age-structured population with density-dependent recruitment requires that at low population densities, each individual produces on average at least one successful offspring within its lifetime (Hastings and Botsford 2006). Assuming that population density is low enough to ignore density-dependent factors, White (2010) showed that this requirement can be expressed as

$$\alpha\lambda_{\mathbf{D}}\text{logit}^{-1}(\theta)LEP \geq 1 \quad (5)$$

where $\lambda_{\mathbf{D}}$ is the leading eigenvalue of the dispersal matrix $\mathbf{D}$ and *LEP* is lifetime egg production, calculated as the sum of the product of survival to age a and fecundity at age a over all ages A.

The basic effect of fishing is to reduce *LEP*. For convenience we express both *LEP* and *SSB* as values relative to the maximum unfished value. The units of all other variables, such as α, are also scaled accordingly. Therefore the persistence threshold in Equation 5 can be expressed as

$$LEP \geq 1/\alpha\lambda_{\mathbf{D}}\text{logit}^{-1}(\theta) \quad (6)$$

The quantity $1/\alpha\lambda_{\mathbf{D}}\text{logit}^{-1}(\theta)$ is referred to as the Critical Replacement Threshold (CRT). The CRT is mathematically related to the Goodyear compensation ratio and the steepness parameter, both of which are often used in fisheries models (White 2010); the CRT is interpreted as the minimum *LEP* required for population persistence. In order to keep our analysis general—rather than specific to kelp rockfish—we express fishing effort in terms of the *LEP* it produces, and parameterize α so that CRT = 0.25 in all model runs (cf. White et al. 2010b; note that White et al. referred to the scaled value of *LEP* as *FLEP*, the fraction of unfished lifetime egg production). In this way, the level of fishing is expressed relative to the persistence threshold, and results would be similar across species for the same value of *LEP* relative to CRT.

Simulated observations of stochastic larval survival

In all simulations described here, we assume that past observations of $S(t)$ and $\phi(t)$ had been made over some period with relatively constant larval production, so that estimating $\theta(t)$ over that period was possible. Therefore we now possess an estimate of the means, $\bar{\theta}$ and $\bar{\phi}$, and standard deviations, s_θ and s_ϕ, of $\theta(t)$ and $\phi(t)$ as well as

an estimate of the linear relationship (including an estimate of the correlation coefficient ρ) between $\theta(t)$ and $\phi(t)$. We further assume that interannual variation in $\phi(t)$ and $\theta(t)$ is such that autocorrelation in those time series is negligible. If larval production varied greatly in the past, estimates of the parameters of $\theta(t)$ and $\phi(t)$ would be biased because variation in $S(t)$ due to production will be incorporated into estimates of s_θ, inflating it. As such, one should be cautious when estimating $\theta(t)$ and $\phi(t)$, and detrending or other processing of $S(t)$ may be necessary.

For clarity it will become important to distinguish between observed values of $\theta(t)$, $\phi(t)$, and $\mathbf{N}(t)$, and values that are simulated from other sources, which we denote with the 'prime' symbol. For example, given an observed vector of physical proxy values $\boldsymbol{\phi}$, we can simulate a corresponding time series $\boldsymbol{\theta}'$ such that $\boldsymbol{\phi}$ and $\boldsymbol{\theta}'$ have correlation ρ. Predicted population densities simulated using $\boldsymbol{\theta}'$ are denoted $\mathbf{N}'$ and predicted spawning stock biomass is $\mathbf{SSB}'$.

A goal of this analysis was to represent the uncertainty in $\theta'(t)$, introduced by the imperfect match between $\theta(t)$ and the proxy $\phi(t)$. We did this by simulating multiple time series $\boldsymbol{\theta}'$ for a given set of observations $\boldsymbol{\phi}$; each simulated $\boldsymbol{\theta}'$ represented one possible set of values with correlation ρ to $\boldsymbol{\phi}$, and by simulating population dynamics for each $\boldsymbol{\theta}'$ we obtained a distribution of possible outcomes $\mathbf{N}'(t)$. To simulate vector $\boldsymbol{\theta}'$ with correlation ρ to vector $\boldsymbol{\phi}$, we first assumed that the linear relationship between $\theta(t)$ and $\phi(t)$ is used to produce $\hat{\boldsymbol{\theta}}$, an estimate of $\boldsymbol{\theta}$ that does not account for the correlation $\boldsymbol{\rho}$ between the two variables (for simplicity we let $\hat{\boldsymbol{\theta}} = \boldsymbol{\phi}$, but this does not affect the results). We then used the following procedure to obtain simulated vectors $\boldsymbol{\theta}'$:

$$\boldsymbol{\theta}'' = \left[\hat{\boldsymbol{\theta}} - \bar{\hat{\boldsymbol{\theta}}}\right] \rho + R(0,s_\theta)[1-\rho^2]^{0.5}$$

$$\boldsymbol{\theta}' = \boldsymbol{\theta}'' - \bar{\boldsymbol{\theta}}'' + \bar{\hat{\boldsymbol{\theta}}}\, \rho + \bar{\theta}\,(1-\rho) \qquad (7)$$

where $R(0,s_\theta)$ is a vector of the same length as $\boldsymbol{\phi}$ containing values drawn from a normal distribution with mean 0 and standard deviation s_θ. The first step produces a set of values with the correct standard deviation and correlation coefficient; the second step ensures that the mean of $\boldsymbol{\theta}'$ approaches the mean of $\hat{\boldsymbol{\theta}}$ as ρ increases. The result of this is that if ρ is near 1, $\boldsymbol{\theta}'$ converges on $\hat{\boldsymbol{\theta}}$. When ρ is near 0, $\boldsymbol{\theta}'$ is simply a random normal distribution with mean $\bar{\theta}$ and standard deviation s_θ, the best available prior estimates for those quantities. Note that in this effort we are accounting only for process error in $\boldsymbol{\phi}$ and error introduced by the strength of correlation ρ (represented by the distribution of $\boldsymbol{\theta}'$); we do not directly consider the effects of observation error in any of these processes or in the measurement of $\mathbf{N}(t)$.

In all cases where $\mathbf{N}'(t)$ is simulated, we also simulated an 'actual' value, which we denoted $\mathbf{N}^\star(t)$, so the accuracy and precision of the distribution of $\mathbf{N}'(t)$ could be estimated by comparison to $\mathbf{N}^\star(t)$. $\mathbf{N}^\star(t)$ was simulated by initializing the model in year $t = -50$ at the deterministic equilibrium (using $\theta(t) = \bar{\theta}$), then running forward in time with a time series $\boldsymbol{\theta}$ generated from random draws from a normal distribution with parameters $\bar{\theta}$ and s_θ. In the simulations presented here, $\bar{\theta}$ was held at a constant value of 0.5. The correction applied in Equation 6 ensures that the results are insensitive to the level of larval survival, because collapse depends only the relative values of *LEP* and CRT. For the sake of generality we describe variation in θ using the coefficient of variation, cv_θ, which is equal to $s_\theta / \bar{\theta}$. We considered values of cv_θ ranging from 0.1 (nearly deterministic) to 10, a range that brackets the observed level of interannual variability in recruitment reported by Caselle et al. (this issue) and Shanks et al. (this issue). Both studies reported levels of variability in recruitment with a coefficient of variability greater than 1; this is not directly comparable to cv_θ as we have defined it, but we know of no studies that have directly reported estimates of temporal variability in larval survival.

Nonspatial model

We first consider the case of a fished population managed in a conventional manner, i.e., assuming that the entire population in a geographical region is a well-mixed unit. As such, there is only a single subpopulation in the models in Equations 1–4 ($n = 1$), and the dispersal matrix $\mathbf{D}$ is a scalar with value 1.

The management scenario is thus: we presume that we are in year $t = 0$. The population has been fished for 30 years at level LEP_{pre}. In year $t = 0$, managers decide to adjust management in order to change *LEP* to one of several possible new values, LEP_{post}. We assume LEP_{pre} can be calculated empirically (e.g., O'Farrell and Botsford 2005), but it is difficult to manage fishing mortality, F, such that a precise value of LEP_{post} will be obtained (note that *LEP* as we have defined it here is equivalent to Spawning Potential Ratio, SPR, as used in the fisheries literature).

In practice, groundfish fisheries on the Pacific coast typically utilize control rules based on spawning biomass rather than *LEP* (or SPR) directly. The overall management target is a value of F that approximates maximum sustainable yield, F_{MSY}. For a particular value of CRT, F_{MSY} is obtained at a particular SPR; in turn, a target value of *SSB* (relative to unfished) is used as a proxy for SPR_{MSY}. For many Pacific groundfish, the target is SPR = 50% of unfished, and the spawning biomass target is 40% of unfished (Ralston 2002; Punt and Ralston 2007). Stocks which decline more than this spawning biomass

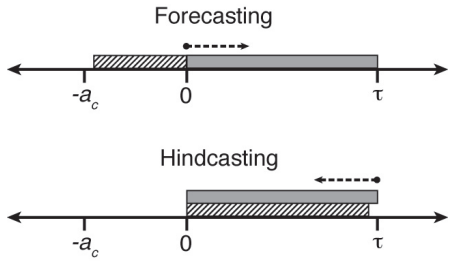

Figure 1. Diagram illustrating difference between forecasting and hindcasting predictions. In the forecasting approach, an observer in year 0 uses information on ϕ from years $t < 0$ (hatched region) to predict population dynamics in the years $0 > t \geq \tau$ (gray region). In the hindcasting approach, an observer in year τ uses information on ϕ from years $t \geq 0$ to predict population dynamics in the years $0 > t \geq \tau$.

target are said to be overfished and the fishery may be curtalied during a stock rebuilding phase. Henceforth we will express spawning biomass as a proportion of the unfished maximum (this is often referred to as 'spawning depletion'). With CRT = 0.25, MSY will actually occur at approximately $LEP = 0.27$ and $SSB = 0.35$. With those equivalencies in mind, we report *SSB* as the response variable in model analyses in order to approximate the type of data that would be used in actual management scenarios.

Forecasting model. In the forecasting scenario, we simulated a decision analysis process at year $t = 0$ and project the outcome (in spawning depletion) of different LEP_{post} targets at years $t = 1, 2, \ldots 10$. These estimates would provide decision makers with estimates (and prediction intervals) of which values of LEP_{post} would produce the desired change in spawning depletion within certain time windows. This type of analysis would typically make forecasts over time periods greater than 10 years, but the shorter window is suitable for our purposes.

The first difficulty encountered in making this type of short-term projection is that the starting conditions, i.e., the full vector $\mathbf{N}(0)$, must be specified, even though the age classes younger than a_c are unobserved. Those pre-recruit age classes depend on the values of $\theta(t)$ at times $(-a_c) \leq t < 0$. To obtain the best estimate of $\mathbf{N}(0)$, we first used the values of M and F_{pre} to back-calculate $\mathbf{N}'(-a_c - 1)$ (i.e., $a_c + 1$ years in the past) from age classes $a > a_c$ in $\mathbf{N}^{\star}(0)$ (as mentioned earlier, an 'actual' time series of $\mathbf{N}^{\star}(t)$ was simulated first). This method leaves the age classes $A - a_c$ to A in $\mathbf{N}'(-a_c - 1)$ empty. We then obtain $\theta'(t)$ from $\phi(t)$ for the period $-(a_c + 1) \leq t < 0$, and use those values of $\theta'(t)$ and the starting conditions $\mathbf{N}'(-a_c - 1)$ to simulate dynamics forward for a_c years to obtain a full estimate of all age classes in $\mathbf{N}'(0)$ (fig. 1). Values for $a \geq a_c$ in $\mathbf{N}'(0)$ are then replaced with the actual values observed in $\mathbf{N}^{\star}(0)$.

To forecast forward in time from $\mathbf{N}'(0)$, we simulated 100 different time series $\boldsymbol{\phi}^{\star}$ for $t = 0, 1, \ldots 9$ using random draws from a normal distribution with mean $\bar{\phi}$ and standard deviation s_θ. For each time series $\boldsymbol{\phi}^{\star}$ we simulated 100 different predicted time series $\boldsymbol{\theta}'$, given a particular value of ρ. We also simulated an additional time series $\boldsymbol{\theta}^{\star}$ that was designated the 'actual' time series. This produced a distribution of 100 possible values of $\mathbf{N}'(t)$ for years $t = 1$ to 10 for comparison to a single 'actual' $\mathbf{N}^{\star}(t)$, repeated for 100 different realizations of the $\boldsymbol{\phi}^{\star}$ and $\mathbf{N}^{\star}(t)$ time series. This procedure was executed for a range of values of LEP_{pre} and cv_θ in order to represent the effects of prior management and environmental variation. For each combination of LEP_{pre} and cv_θ, we also modeled a range of values of LEP_{post} to simulate a decision analysis process wherein managers are presented with the range of possible outcomes for each management alternative.

Hindcasting model. We suppose that in year $t = \tau$ in the future there is a desire to manage adaptively by determining whether the management action taken at $t = 0$ met expected goals (i.e., whether the chosen target value of LEP_{post} produced the desired change in spawning biomass). In this case the difficulty is distinguishing the effects of stochastic variability in recruitment from changes in spawning biomass due to management. Therefore we simulate a "hindcasting" procedure, in which an observer at year τ models dynamics between years zero and τ to obtain a projection of the expected *SSB* at τ, accounting for recruitment variability in the intervening years (fig. 1). Note that we refer to this as hindcasting, but the hindcasting occurs from year τ ("future") back towards year 0 ("present") rather than from year 0 back towards years $t < 0$ ("past").

The population density $\mathbf{N}(\tau)$ is now observable (at least for ages $a \geq a_c$), but $\boldsymbol{\theta}$ for years $0 - \tau$ is unknown. We estimated the distribution of $\mathbf{N}'(\tau)$ using a procedure similar to that in the forecasting model. Starting with the same estimate of density at $\mathbf{N}'(0)$ used in the forecasting model, the observed values $\boldsymbol{\phi}$ for years 0 to $(\tau - 1)$ were used to simulate 100 different possible time series $\boldsymbol{\theta}'$, which were used in turn to obtain a distribution of values for $\mathbf{N}'(\tau)$. As before, the values of $\mathbf{N}'(\tau)$ for ages $\geq a_c$ were constrained to be equal to the observed values in $\mathbf{N}^{\star}(t)$, and the entire procedure was performed for 100 different time series of $\mathbf{N}^{\star}(t)$.

Together these forecasting and hindcasting analyses are similar to a management strategy evaluation, in that we consider the ability of managers to make correct inferences about fishery stock status in the face of environmental process error. However, unlike typical management strategy evaluations analyses, we only consider the consequences of a single change in management strategy (at time $t = 0$) and examine both the success of decision analysis at that time and managers' ability to detect the consequences of that action at an arbitrary point in the future.

Spatial model

We then considered the case of spatial management, including the use of no-take marine protected areas (MPAs). This introduces several changes into the model: **D** is now an $n \times n$ matrix of dispersal probabilities. We assumed that demographic parameters were constant across all n populations, and that the fishing rate, F, was also constant across space (except that $F = 0$ inside any MPA). Adult fish can move inside home ranges, so fish that settle inside MPAs can move across MPA boundaries and experience fishing pressure. We assumed that home range movement follows a Gaussian distribution with mean 0 and standard deviation $h/2$, so that fish spend 95% of their time within a radius h of their settlement location (cf. Moffitt et al. 2009; Freiwald 2009). Then the fishing pressure of a fish with home range centered at spatial cell i is given by

$$\widehat{F_i} = \frac{1}{h\sqrt{\pi/2}} \int_{-\infty}^{\infty} c_x F_x \exp\left[- \frac{4(x - x_0)^2}{h^2} \right] dx \qquad (7)$$

where $\widehat{F_i}$ is the effective fishing rate experienced by an individual with a home range centered at spatial cell i, F_x is the fishing rate at location x, $c_x = 0$ for reserves and 1 for fished areas, and x_0 is the center of cell i, and the integration is made over one-dimensional space x. The effective fishing rate $\widehat{F_i}$ was then used to calculate LEP_i and the expected fishery yield of recruits settling at each cell i. This is similar to the approach taken by Moffitt et al. (2009), but with a Gaussian rather than uniform distribution of home range movement.

We assumed a spatial domain consisting of a linear coastline with homogenous habitat. The coastline was simulated as a repeating unit of 40 spatial cells representing 40 km of coastline; dispersing larvae and adult home ranges wrapped around the edge of the domain, eliminating edge artifacts and making the coastline effectively infinite (very similar results would be obtained on a very long non-infinite coastline, but our approach is computationally much simpler). In principle, model results should be sensitive to this assumption; if the domain had absorbing boundaries then a species with long larval dispersal distances should lose many larvae off of the edge of the domain. This would results in lower overall larval replenishment and make it less likely that the species would persist. However, as described above, the model is parameterized such that the persistence threshold is precisely given by Equation 6, regardless of losses due to larval survival or transport processes. Therefore, we have avoided any sensitivity to assumptions about domain boundaries.

While MPA size and spacing have been examined for protected populations (e.g., White et al. 2010b), we were concerned with the effects of recruitment variability, so we considered only two different MPA configurations. The primary set of results were generated for MPAs that conformed to size and spacing guidelines from the California Marine Life Protection Act initiative (CDFG 2008): MPAs were 10 km wide and separated by 30 km of fished area. This produced MPAs that covered 25% of the coastline. For comparison with a smaller MPA scenario, we also simulated a coastline with 3 km wide MPAs, covering 7.5% of the 40 km coastline.

Larval dispersal was assumed to be purely diffusive and described by a Gaussian dispersal kernel with zero mean displacement a standard deviation d. Hereafter, d is referred to as "dispersal distance." For this type of model, the nature of deterministic population persistence depends on the spatial scale of movement relative to MPA size: if the scale of larval dispersal is much smaller than the scale of MPA width, then populations tend to exhibit self-persistence and MPAs are self-sustaining units. If the spatial scales of larval dispersal and/or adult home range movement are much larger than MPAs, then persistence depends on connectivity over space across multiple generations, termed a network effect, and is more sensitive to the fraction of the coastline in MPAs than to MPA size (Hastings and Botsford 2006; Moffitt et al. 2009; White et al. 2010). To capture this range of model behavior, we modeled four different life history scenarios, including each combination of long and short adult and larval dispersal distances ($d = 5$ km or $d = 40$ km and $h = 0.1$ km or $h = 10$ km).

In addition to the case of a simple homogenous coastline, the dynamics of which are well understood in deterministic models (e.g., Botsford et al. 2001; White et al. 2010b), we also considered a case in which the coastline has a recruitment 'hotspot' or retention zone. It is generally recommended that MPAs be placed in locations with high recruitment (e.g., Halpern and Warner 2003; Roberts et al. 2003) and there is some evidence from models that this strategy may be successful (White et al. 2010a), but such hotspots could amplify the effects of variable recruitment. We modeled the recruitment hotspot scenario by creating an oceanographic retention zone following the procedure for scenario "B" in White et al. (2010a): inside the retention zone—which was assumed to be contiguous with the MPA—the standard deviation of the Gaussian dispersal kernel was $d/2$ instead of d. This produces a higher degree of larval retention (and less spillover) in that area. We did not consider the case of spatial variation in recruitment, since recruitment patterns of nearshore California fishes are often coherent over large spatial scales within a year, even if the overall magnitude varies (Caselle et al., this issue).

We considered two types of output in the spatial model, both of which approximate commonly used measures of MPA effectiveness (Lester et al. 2009). The first

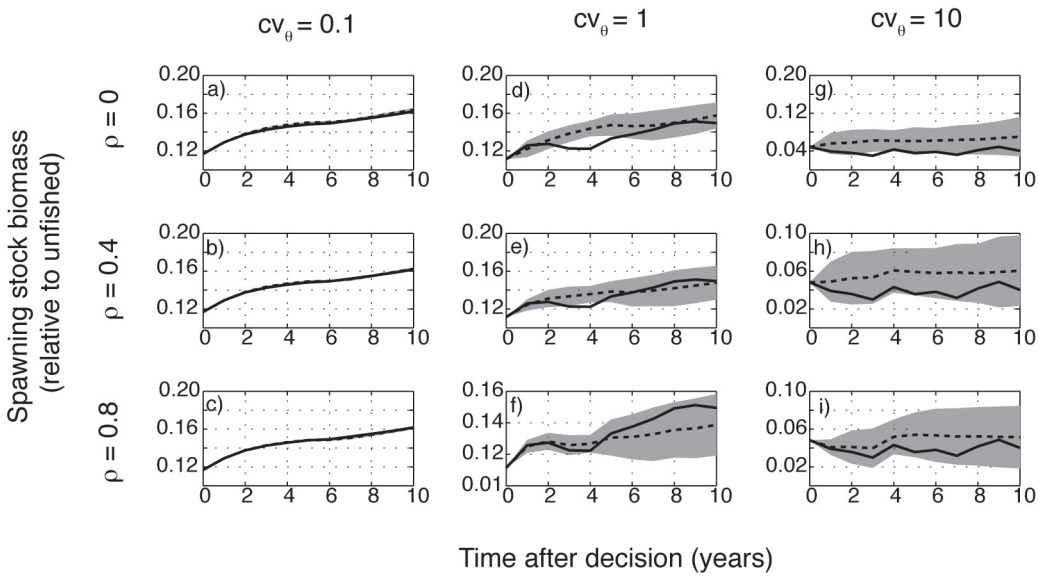

Figure 2. Time series from the nonspatial forecasting model. Panels depict the time series of actual spawning stock biomass (*SSB**; solid line) as well as the mean (dashed line) and 95% prediction interval (gray area) of model projections (*SSB*') for a particular combination of variability in larval survival (cv_θ) and the correlation (ρ) between actual larval survival and a physical proxy. Model projections are based on an initial observation of the fished population at time $t = 0$; for larger values of ρ, the model projections incorporate increasingly better proxy-derived estimates of the initial density of unfished age classes. The population was being overfished prior to $t = 0$ ($LEP_{pre} = 0.2$) and is then switched to sustainable fishing ($LEP_{post} = 0.35$).

is the log of the ratio of *SSB* after:before MPA implementation for a location inside the MPA. This measure captures the trajectory of increase (or decrease) in biomass inside the MPA relative to the baseline situation in $t = 0$. We report the log after:before *SSB* ratio for location $x = 5$, in the center of the MPA. The second metric is the log of the ratio of SSB at a location inside the MPA to *SSB* at a location outside the MPA. This metric is an attempt to account for large-scale environmental variability (such as variability in $\theta(t)$) that might dampen the effects of the MPA over short time scales (as measured by the after:before comparison), under the assumption that a well-performing MPA will still contain higher biomass than a fished location. In the 10 km MPA scenario we report this log inside:outside ratio for locations $x = 5$ (inside) and $x = 25$ (outside); for the 3 km MPA scenario we used locations $x = 2$ (inside) and $x = 17$ (outside).

The management scenario for the spatial model is similar to that in the nonspatial model: we assume that a population has been fished for 30 years at the level $LEP_{pre} = 0.2$ (i.e., overfished). In year $t = 0$ (the present day), managers choose to implement an MPA network along the coastline. At the same time, they also choose a new target value of LEP_{post} for the remaining fished areas of the coast. The level of fishing outside the MPA can greatly affect MPA performance, especially for species with large scales of larval or adult movement (White et al. 2010b). Thus projections of MPA performance must specify the expected level of LEP_{post}, and adaptive management of MPAs must account for the observed increase in SSB relative to that projection. Therefore, the spatial model was run for 3 values of LEP_{post} (0.2, 0.35, 0.5 ranging from overfished to sustainably fished), just as in the nonspatial model. Model performance was evaluated in terms of its ability to predict the correct log *SSB* ratio and distinguish among alternative log *SSB* ratios.

RESULTS

Nonspatial model

An example of the population dynamics forecasting model is provided in Figure 2, with lifetime egg production prior to $t = 0$, LEP_{pre}, equal to 0.2, and then $LEP_{post} = 0.35$ after $t = 0$, for a range of values with the correlation strength of the proxy, ρ, and variability in larval survival, cv_θ. In each panel, the range of projected outcomes for $t = 1$–10 years in the future is shown relative to the actual trend in spawning stock biomass, $SSB^\star(t)$, for a typical realization of actual larval survival values $\boldsymbol{\theta}$. When cv_θ was very low, dynamics were nearly deterministic, so incorporating information from the physical proxy did not improve model forecasting substantially (fig. 2a–c). Projections of $SSB'(t)$ had narrow prediction intervals that usually contained the actual value $SSB^\star(t)$, even when $\rho = 0$ (fig. 2a). As cv_θ increased, the proxy afforded a larger improvement in predictive skill (fig. 2d–i). For $cv_\theta = 1$, the predicted range of $SSB'(t)$ deviated from the actual value of $SSB^\star(t)$ in the absence of a proxy ($\rho = 0$); that is, the model incorrectly forecasted dynamics just 3–4 years into the future (e.g., fig. 2d). However, the range of model projections followed $SSB^\star(t)$ much

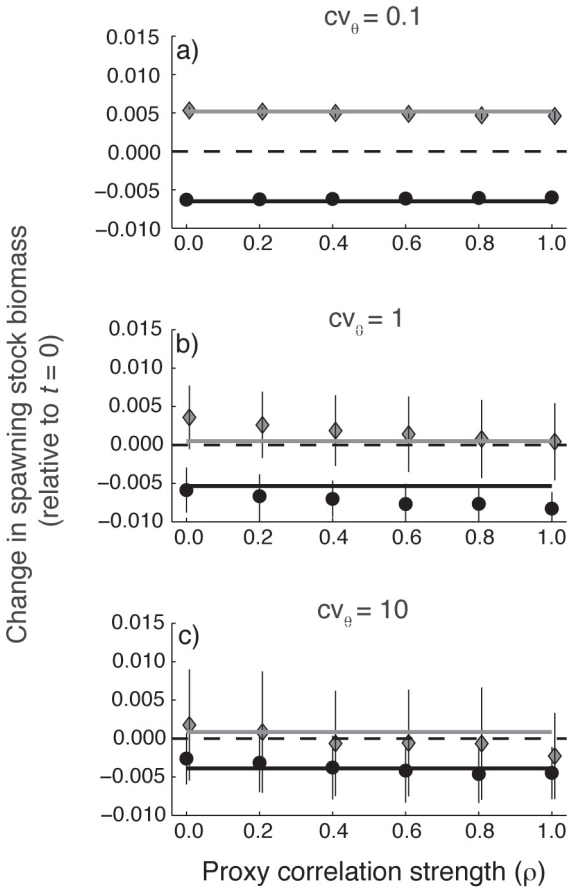

Figure 3. Results from the nonspatial forecasting model showing the deviation of model projections from actual values. Points depict the projected spawning stock biomass (*SSB*') at t = 10 years after fishery management switched from LEP_{pre} = 0.2 (overfishing) to an alternative level of fishing (LEP_{post}): 0.5 (light gray diamonds) or 0.2 (black circles). Projections are shown for a range of values of the correlation ρ between actual larval survival and a physical proxy. Error bars indicate 95% prediction interval for model projections. Solid lines indicate actual *SSB** values for the corresponding value of LEP_{post}. The level of variability in natural survival, cv_θ, differs among panels as indicated. *SSB* values are presented as deviations from *SSB* at time t = 0; no deviation indicated by dashed horizontal line. For decision analysis at t = 0, the quantity of interest is the degree of overlap in the range of projected outcomes for different levels of LEP_{post}. For adaptive management at t > 0, the quantity of interest is whether the range of projected outcomes for a particular LEP_{post} contain the actual value.

more closely with higher values of ρ. Similar patterns held for a much higher level of variability in survival, cv_θ = 10, but the range of projected model outcomes was much higher overall in this case, so projections were less precise but the range of values usually contained $SSB^\star(t)$ (fig. 2g–i). Regardless of the value of cv_θ and ρ, the improvement in predictive skill afforded by the proxy fell off after approximately 5 years, as indicated by a widening of the prediction interval around the model projection. This corresponds to the age at recruitment to the fishery, a_c. After a_c years, all of the pre-recruit cohorts present at t = 0 and estimated from observations of the physical proxy ϕ prior to t = 0 had entered the fishery. After this point ($t > a_c$), the proxy cannot provide any additional information on pre-recruit cohorts, because they were all spawned after t = 0. Consequently, the range of model outcomes became wider. Note also that simulations with low noise ($cv_\theta \leq 1$) exhibited an overall increase in *SSB*, consistent with a decrease in fishing switching from LEP_{pre} = 0.2 to LEP_{post} = 0.35, whereas in the higher-noise scenario (cv_θ = 10) this switch did not produce an obvious increase in *SSB*.

The predictive skill of model projections has two important components. First, projections must be sufficiently precise (i.e., narrow prediction intervals) so that the outcomes of alternative management scenarios (LEP_{post}) can be distinguished within a decision analysis setting at time t = 0. Otherwise, model uncertainty overwhelms the scope of potential management outcomes. Second, projections must be sufficiently accurate that the prediction intervals of projections for a particular management scenario (LEP_{post}) encompass the actual value for that management outcome, and not the value for other management outcomes. If not, the model might indicate that the observed spawning stock biomass corresponded to an incorrect level of LEP_{post}. That is, the model would be unable to account for process error in the dynamics, and would make an incorrect prediction.

To illustrate these two components of model skill, Figure 3 shows the mean and 95% prediction interval for forecast model projections for a range of values of LEP_{post}, correlation strength ρ and variability in larval survival cv_θ at 10 years post-decision, again using a single model realization for illustration (LEP_{pre} = 0.2). When variability in survival was low and dynamics were nearly deterministic (fig. 3a), model projections for each value of LEP_{post} did not overlap and closely matched the actual value at all time steps, regardless of the correlation strength of the proxy. These results also illustrate the general deterministic trend that $LEP_{post} < 0.35$ led to additional declines in *SSB* while $LEP_{post} \geq 0.35$ produced an increase in *SSB*. This result may be relevant not only for the rockfish model depicted in this case but may be more generally applicable.

For an intermediate level of variability (cv_θ = 1; fig. 3b), the prediction intervals of model projections for different values of LEP_{post} rarely overlapped, even for low correlation strength ρ. However, higher values of ρ produced a closer match between the model projection spawning stock biomass *SSB*' and the actual value $SSB^\star$.

When there was much greater natural variability in larval survival (cv_θ = 10; fig. 3c), the 95% prediction intervals for $SSB'(t)$ under different values of LEP_{post} overlapped considerably for low values of the correlation strength ρ, so that a decision analysis effort at t = 0 would predict that it is impossible to distinguish the effects of very different fishing rates on *SSB* over this time scale. Similarly, the prediction interval for a given

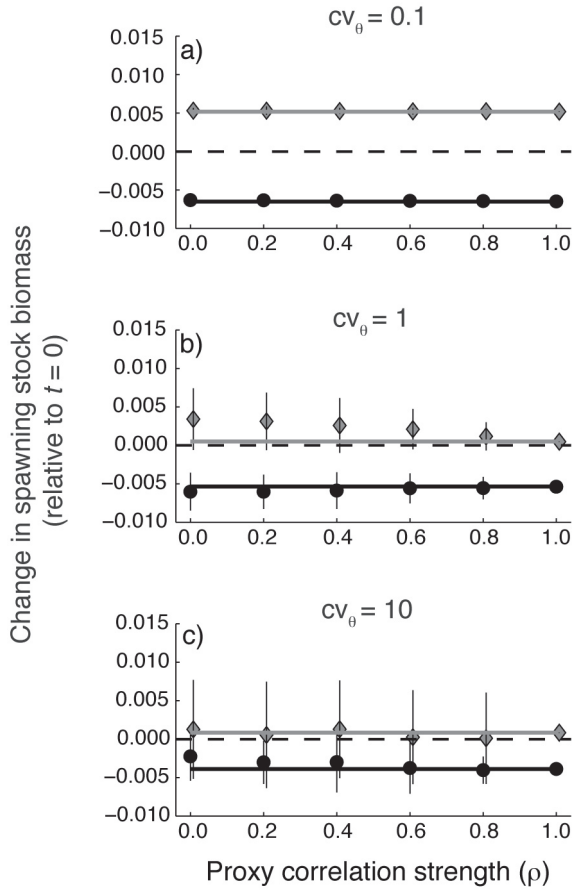

Figure 4. Results from the nonspatial hindcasting model showing the deviation of model projections from actual values. Each series of points depicts the projected spawning stock biomass (*SSB*') at t = 10 years after fishery management switched from LEP_{pre} = 0.2 (overfishing) to an alternative level of fishing (LEP_{post}): 0.5 (light gray diamonds) or 0.2 (black circles). Projections are shown for a range of values of the correlation ρ between actual larval survival and a physical proxy. Error bars indicate 95% prediction interval for model projections. Solid lines indicate actual *SSB** values for the corresponding value of LEP_{post}. The level of variability in natural survival, cv_θ, differs among panels as indicated. *SSB* values are presented as deviations from *SSB* at time t = 0; no deviation indicated by dashed horizontal line. For decision analysis at t = 0, the quantity of interest is the degree of overlap in the range of projected outcomes for different levels of LEP_{post}. For adaptive management at t > 0, the quantity of interest is whether the range of projected outcomes for a particular LEP_{post} contain the actual value.

projection overlapped multiple values of $SSB^\star(t)$. Thus it would be impossible to determine from examining *SSB* at year 10 whether the desired value of LEP_{post} was being achieved, because uncertainty about the variability in recruitment would be too large. However, the prediction intervals on model projections diminished with increasing ρ, and both the accuracy and precision of model projections were much greater for $\rho > 0.8$.

Interestingly, over longer time scales (e.g., t = 10), it was possible for a strong correlation between the proxy and larval survival to actually introduce error into the model projection and produce a greater deviation from the actual value. This appears to occur because the relatively narrow prediction intervals on *SSB*' during the period t = 0 to $t = a_c$ constrain the model trajectory in later years, and slight errors during that early period can propogate through time, producing larger errors later (compare fig. 2e to 2f).

Results similar to those shown in Figure 3 for the forecasting model are also obtained in the hindcasting model (fig. 4), in which values of the physical variable $\phi(t)$ from years t = 1–10 are used as a proxy for $\theta(t)$ in those years. The notable differences are that prediction intervals around model projections are generally smaller, and projections always converge towards $SSB^\star$ as ρ approaches 1.

The general patterns illustrated in Figures 2–3 are summarized for 100 different realizations of the actual larval survival time series $\boldsymbol{\theta}^\star$ in Figure 5. In order to summarize the distribution of model projections for each model realization (i.e., each set of actual values $\boldsymbol{\theta}^\star$), the mean and standard deviation of predicted *SSB*' were compared to the actual value $SSB^\star$ using a standard normal deviate: $z = (\overline{SSB'} - SSB^\star)/s_{SSB'}$. We then calculated the average z-statistic across all model realizations for a particular combination of LEP_{pre}, LEP_{post}, variability in larval survival cv_θ, correlation strength ρ, and time t. The p-value corresponding to this z-statistic indicates the probability that the actual value of $SSB^\star$ falls within the distribution of projected *SSB*' values; that is, the accuracy of the projections. Examination of these p-values (fig. 5a–e) indicates that model accuracy is maximal for $\rho > 0.6$ (note that the contour lines grow closer just above $\rho > 0.6$) and $t \le 4$ (recall that the age at recruitment to the fishery, a_c, is 4). The p-values fall off sharply below the value of $\rho > 0.6$ over short time scales. Over longer time scales ($t > 4$), model accuracy is relatively constant across all values of ρ, but decreases somewhat for higher values of ρ after t = 8. This general pattern holds across all levels of variability cv_θ, and correspond to the patterns noted in Figure 3 for a single model realization.

We also employed the same z-statistic procedure to compare *SSB*' for $LEP_{post} = 0.35$ to the actual value of $SSB^\star$ for $LEP_{post} = 0.2$. In this case, the p-value measures the probability that an incorrect value of $SSB^\star$ would fall within the distribution of *SSB*' values, that is, the precision of the model projections. In this case, the p-values were uniformly low across all values of correlation strength ρ for low levels of natural variability (fig. 5f–h). For higher levels of variability ($cv_\theta \ge 5$), the pattern of this metric of model skill roughly matched that for the comparison of *SSB*' to the correct $SSB^\star$: p-values were high for low values of ρ early in simulations (indicating high overlap with the incorrect value) and moderate ($p \sim 0.15$) for most values of ρ in later years (fig. 5i–j). The major difference from the comparison shown in Figure 4a–e is that model skill remained high for high values of ρ ($\rho \ge 0.8$) across all time-steps.

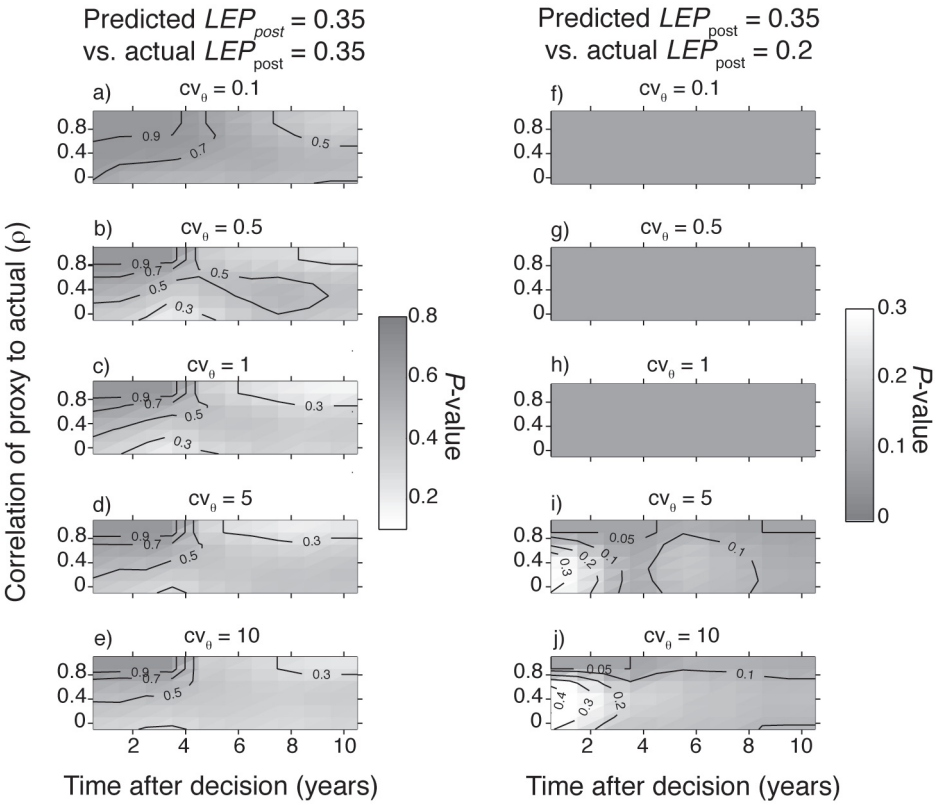

Figure 5. Results from multiple realizations of the nonspatial forecasting model showing the predictive skill of model projections. Model results were summarized as the standard normal deviate (*z*-statistic) for the deviation of the mean model projection from the correct actual value (a–e) or the actual value for an alternative level of LEP_{post} (f–j). Each *z*-value was then translated into a *p*-value, representing the probability that the range of model projections contains the correct value (a–e) or an incorrect alternative value (f–j). Each panel shows the range of outcomes over time after $t = 0$ for increasing values of the correlation of actual larval survival rates to a physical proxy (ρ) and a given level of natural variability in larval survival (cv_θ). Note that shading in panels (a–e) is opposite that in (f–j); in both cases darker values indicate better model performance.

As in the example shown above (fig. 4), the overall behavior of the hindcasting model was similar to that depicted for the forecasting model in Figure 4, but with smaller prediction intervals and thus improved model performance (fig. 6). Additionally, high values of ρ were uniformly advantageous across all time-steps, and did not lead to a decrease in model performance at $t = 10$ (compare upper left corners of Figure 5a–e and Figure 6a–e).

Here we have presented results only for the case of $LEP_{pre} = 0.2$, in which the pre-decision population was undergoing overfishing. Model results for $LEP_{pre} = 0.4$ (sustainable fishing) exhibit nearly identical patterns of model accuracy with respect to ρ, cv_θ, and t, and for brevity we simply state this result without a figure.

Spatial model

An example of the behavior of the spatial model with diffusive dispersal and a 10 km wide MPA is shown in Figure 7. Overall, adult movement (defined by adult home range radius h) had a much greater effect on the spatial pattern of *SSB* than did variation in larval disperal distance (defined by dispersal distance d). Indeed, *SSB* was 3× greater for the model runs with small home range size compared with large (fig. 7a, b), but differed little between the two larval dispersal distances. The apparent lack of an effect of dispersal distance d is because the MPA in these model runs was large enough to be self-persistent for small d and covered enough area to be network persistent for large d (when home range size was small), so the population inside the MPA was persistent in either scenario. However, LEP_{post} did affect overall *SSB*, even inside the MPA, for all movement scenarios. The effects of LEP_{post}, and the tendency for recruitment variability to obscure those effects, were amplified with greater adult movement. Notice that for $LEP_{post} = 0.2$, the large-home-range case was not persistent despite the MPA (i.e., biomass continues to decline after MPA implementation), but with a moderate amount of recruitment variability ($cv_\theta = 1$ in this example) the decline was not immediately evident in all simulations (fig. 7c, d).

The general patterns observed in the diffusive dispersal case were similar to those in the retention zone scenario (fig. 8), although densities within the MPA were slightly elevated by the shorter home ranges and shorter

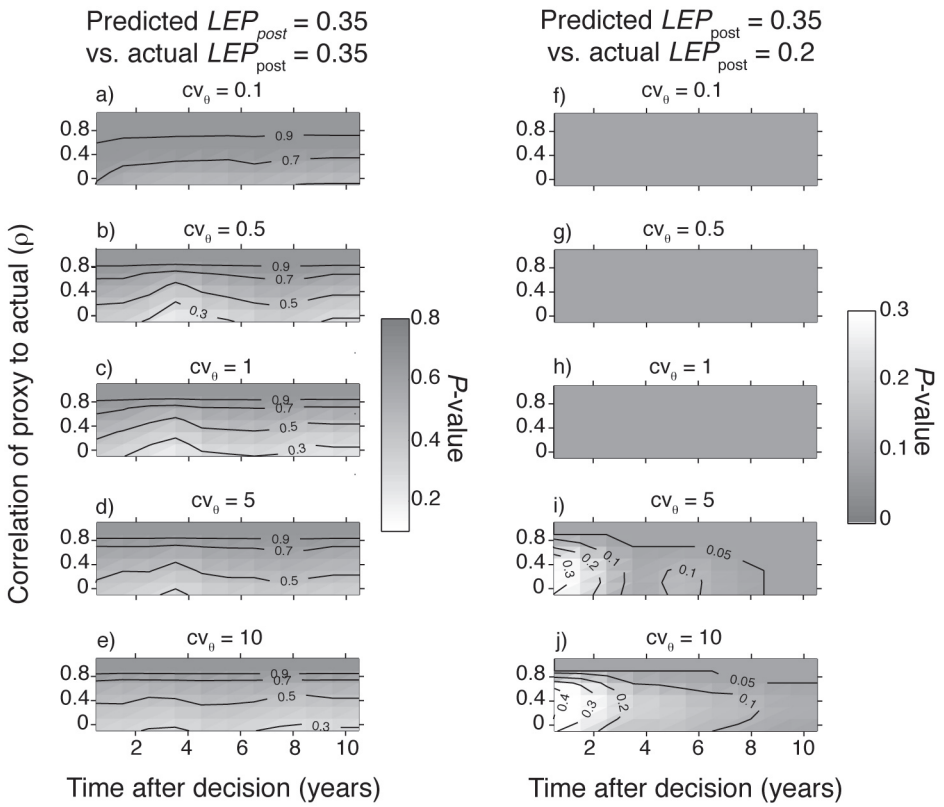

Figure 6. Results from multiple realizations of the nonspatial hindcasting model showing the predictive skill of model projections. Model results were summarized as the standard normal deviate (*z*-statistic) for the deviation of the mean model projection from the correct actual value (a–e) or the actual value for an alternative level of LEP_{post} (f–j). Each z-value was then translated into a *p*-value, representing the probability that the range of model projections contains the correct value (a–e) or an incorrect alternative value (f–j). Each panel shows the range of outcomes over time after $t = 0$ for increasing values of the correlation of actual larval survival rates to a physical proxy (ρ) and a given level of natural variability in larval survival (cv_θ). Note that shading in panels (a–e) is opposite that in (f–j); in both cases darker values indicate better model performance.

larval dispersal distances. Populations with large home ranges were persistent in the $LEP_{post} = 0.2$ case when larval dispersal was short (note the slightly increasing *SSB* in Figure 8c) but not long (fig. 8d); in the former case the additional recruitment afforded by the retention zone inside the MPA was sufficient to offset the fishing of individuals moving outside the MPA boundaries.

Evaluations of MPA performance typically take either or both of two forms: an after:before comparison of biomass within an MPA and an inside:outside comparison of biomass in the MPA relative to that in a fished control. The after:before comparison seeks to determine whether biomass is recovering inside the MPA, but that signal can be obscured by recruitment variability. The inside:outside comparison is intended to control for large-scale variability in recruitment and other processes, but assumes that there is a substantial difference in fishing pressure inside vs. outside. We simulated both of these types of comparisons. An example is given in Figure 9, showing the log ratio of *SSB*' after:before for a location inside the MPA (fig. 9a–c) and log ratio of *SSB*' inside:outside measured at a location in the center of the MPA and the center of the fished area (fig. 9d–f). The general patterns of accuracy and precision of the model projections were similar to those observed in the nonspatial model: the signal of deterministic change in *SSB*' due to LEP_{post} increased over time, that signal was more difficult to detect as recruitment variability (cv_θ) increased, and higher values of ρ increased the precision of model projections. As in the nonspatial model, the increase in precision afforded by the forecast estimate of $\theta(t)$ declined after $t = 5\ \gamma$ ($t = t_c$). The major new pattern evident in the spatial model was that the value of LEP_{post} had a strong effect on the inside:outside ratio (fig. 9d–f) but only a minimal effect on the after:before ratio (fig. 9a–c; there was a slightly greater effect of LEP_{post} in the large home range scenario). There was also a strong effect of adult home range movement on the two response ratios, as summarized below.

As in the nonspatial model, we summarized the accuracy and precision of the spatial model results using *z* statistics to quantify whether A) model projections bracketed the actual value, and B) projections bracketed incorrect values associated with other values of

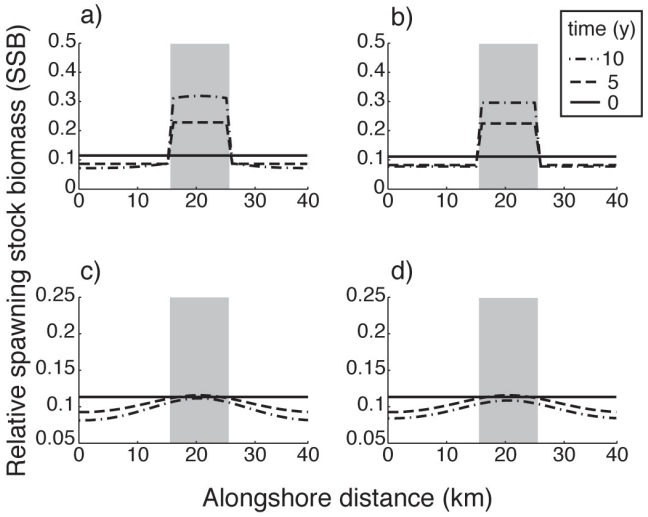

Figure 7. Results from spatial forecasting model with spatially homogenous larval dispersal and a moderate level of variability in larval survival (cv_θ = 1). The mean value (across all simulations) of the actual value of *SSB** (relative to the unfished maximum) at each time is shown for LEP_{pre} = 0.2 and LEP_{post} = 0.2, at t = 0 (solid lines), 5 (dashed lines), and 10 (dot-dash lines) years after MPA implementation. Each panel shows results for a model species with a different combination of larval dispersal distance (d) and home range diameter (h): a) short d, short h (d = 5 km, h = 0.1 km); b) long d, short h (d = 40 km, h = 0.1 km); c) short d, long h (d = 5 km, h = 10 km); d) long d, long h (d = 40 km, h = 10 km). Gray shading indicates location of MPA within the 40 km repeating unit of infinite coastline.

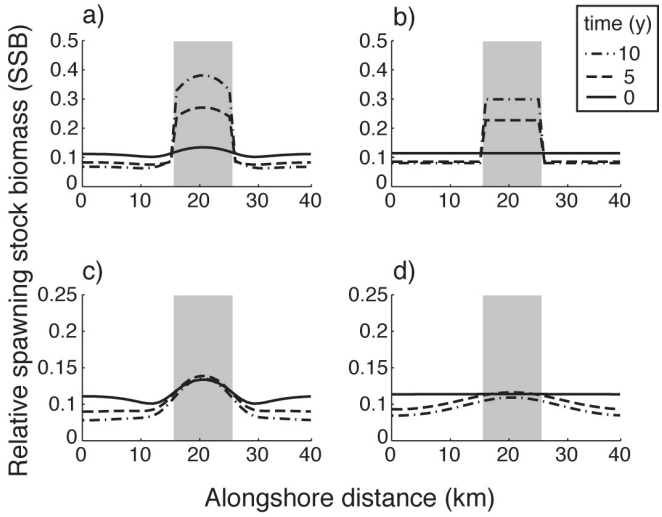

Figure 8. Results from spatial forecasting model with a larval retention zone and a moderate level of variability in larval survival (cv_θ = 1). The mean value (across all simulations) of the actual value of *SSB** (relative to the unfished maximum) at each time is shown for LEP_{pre} = 0.2 and LEP_{post} = 0.2, at t = 0 (solid lines), 5 (dashed lines), and 10 (dot-dash lines) years after MPA implementation. Each panel shows results for a model species with a different combination of larval dispersal distance (d) and home range diameter (h): a) short d, short h (d = 5 km, h = 0.1 km); b) long d, short h (d = 40 km, h = 0.1 km); c) short d, long h (d = 5 km, h = 10 km); d) long d, long h (d = 40 km, h = 10 km). Gray shading indicates location of MPA within the 40 km repeating unit of infinite coastline. The MPA contains the larval retention zone, inside which larval dispersal distance d is reduced by 50%.

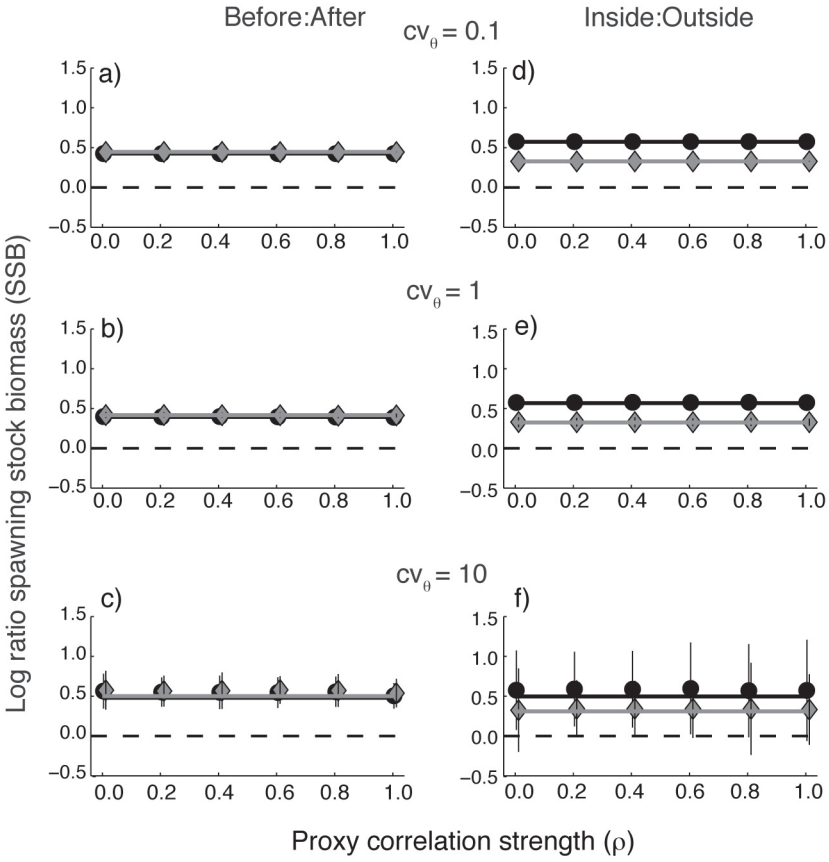

Figure 9. Results from the spatial forecasting model with spatially homogenous dispersal showing the deviation of model projections from actual values. Each series of points depicts the projected spawning stock biomass (*SSB'*) at t = 10 years after MPAs were implemented and fishery management switched from LEP_{pre} = 0.2 (overfishing) to an alternative level of fishing (LEP_{post}): 0.5 (light gray diamonds) or 0.2 (black circles). Projections are shown for a range of values of the correlation ρ between actual larval survival and a physical proxy. Error bars indicate 95% prediction interval for model projections. *SSB* is expressed as (a–c) the log ratio of SSB before:after MPA implementation for a location inside the MPA (t vs t = 0), or (d–f) the log ratio of *SSB* inside:outside the MPA at the same time. Solid lines indicate actual values for the corresponding value of LEP_{post}. The level of variability in natural survival, cv_θ, differs among panels as indicated. These results were obtained using the forecasting model for a species with long larval dispersal distance (d = 40 km) and short adult home range (h = 0.1 km); the MPA was 10 km wide.

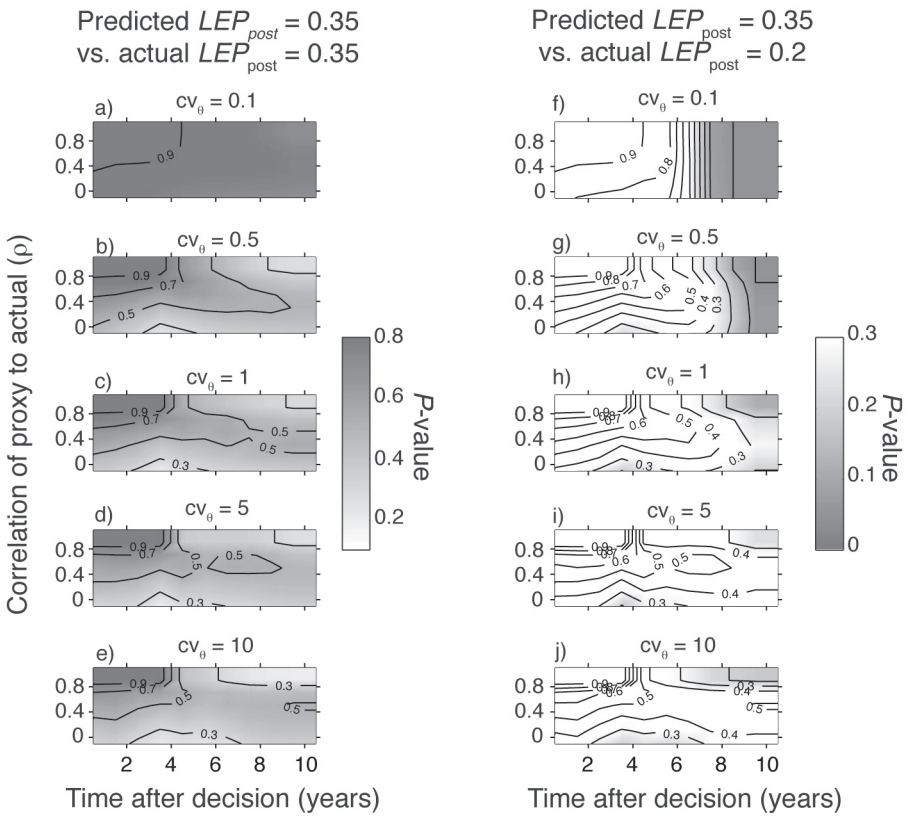

Figure 10. Results from multiple realizations of the spatial model with spatially homogenous dispersal showing the predictive skill of model projections for the ratio of *SSB* after:before MPA implementation. These results were obtained using the forecasting model for a species with long larval dispersal distance (d = 40 km) and short adult home range (h = 0.1 km); the MPA was 10 km wide. Model results were summarized as the standard normal deviate (z-statistic) for the deviation of the mean model projection of the *SSB* ratio for LEP_{post} = 0.35 from (a–e) the correct actual value for that level of LEP_{post}, or (f–j) the actual value for an alternative management scenario with LEP_{post} = 0.2. Each z-value was translated into a p-value, representing the probability that the range of model projections contains the correct value (a–e) or an incorrect alternative value (f–j). Each panel shows the range of outcomes over time after t = 0 for increasing values of the correlation of actual larval survival rates to a physical proxy (ρ) and a given level of natural variability in larval survival (cv_θ). Note that grayscale in panels (a–e) is opposite that in (f–j); in both cases darker values indicate better model performance.

LEP_{post}. Even though the MPAs modeled in these scenarios were big enough to support a persistent population in most cases (regardless of LEP_{post}), the value of LEP_{post} affects the *SSB* inside MPAs (cf. figs. 7–9). An adaptive management evaluation of MPA performance will require a model projection of how much *SSB* should have increased inside (or outside) the MPA. We first examine the results obtained from the diffusive dispersal scenario. There was essentially no effect of larval dispersal distance on the z statistics (data not shown), so we focus on the results for the two home range sizes and long larval dispersal distances (d = 40). For the short home range case (h = 0.1; fig. 10), forecast projections of the after:before *SSB*' ratio always had considerable overlap with the ratio associated with the correct LEP_{post} (fig. 10a–e), although the accuracy was somewhat better for correlation strength $\rho > 0.8$ over short timescales ($t < 5$ y). The distribution of after:before *SSB*' ratios also had considerable overlap with ratios associated with alternative values of LEP_{post} in early years ($t <$ 6 y) for all values of correlation strength ρ and survival variability cv_θ (fig. 10f–j). This lack of precision is a consequence of the minimal deterministic effect of different LEP_{post} values on the after:before ratio in that initial time period. However, in high-noise ($cv_\theta \geq 1$) scenarios, an informative proxy ($\rho > 0.8$) did improve the precision of model projections after t = 8 y (fig. 10h–j). That is, the value of LEP_{post} had a long-term effect on MPA performance, but the trajectories of the after:before ratio associated with different values of LEP_{post} were only distinguishable within a reasonable time scale ($t < 10$ y) when an effective proxy for $\theta(t)$ was used.

The overall model skill in the short home range case was higher when *SSB*' was measured as the inside:outside ratio (fig. 11). Using that metric, forecast projections always had a high degree of overlap with the value associated with the correct LEP_{post} (fig. 11a–e) and very little overlap with ratios associated with alternative values of LEP_{post} (fig. 11f–j), except for very high values of cv_θ (fig. 11i–j). This result suggests that the inside:outside ratio does appear to control for environmental stochasticity when testing for the effects of an MPA. None-

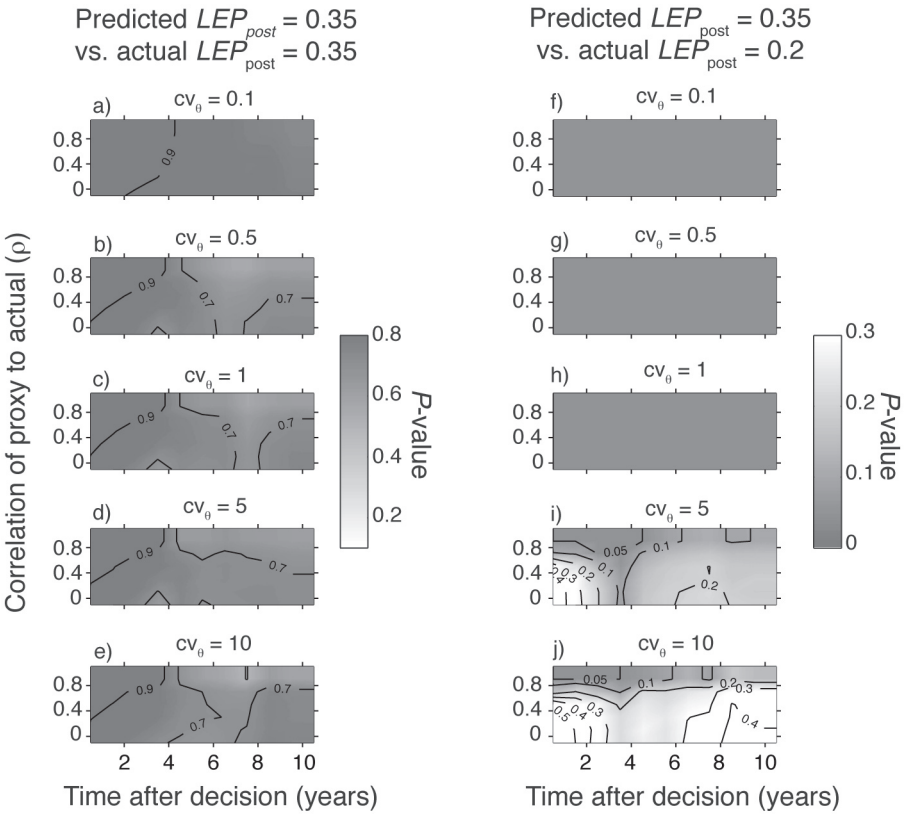

Figure 11. Results from multiple realizations of the spatial model with spatially homogenous dispersal showing the predictive skill of model projections for the ratio of *SSB* inside:outside the MPA. These results were obtained using the forecasting model for a species with long larval dispersal distance (d = 40 km) and short adult home range (h = 0.1 km); the MPA was 10 km wide. Other figure details as in Figure 10.

theless, the forecasts had greater precision in high noise situations ($cv_\theta > 1$) when an effective proxy was used ($\rho > 0.8$; fig. 11i–j).

The accuracy and precision of forecast projections were strikingly different for a species with a large home range (h = 10 km). This is because home range movement dilutes the protection of an MPA, so that the change in biomass inside the MPA is more sensitive to the level of fishing outside (Moffitt et al. 2009), producing a larger, more rapid divergence in *SSB*' among alternative values of LEP_{post}. When forecasting the after:before *SSB*' ratio, projections had far less overlap with the value associated with the actual LEP_{post} (fig. 12a–e) than in the small home range scenario, and use of a proxy with $\rho > 0.8$ yielded considerable improvement in accuracy over timescales shorter than t_c (i.e., $t \leq 4$ years). By contrast, the forecast after:before ratio had much less overlap with values associated with alternative LEP_{post}, and the proxy only improved precision over short time scales ($t < 4$ y) in high-variability scenarios ($cv_\theta > 1$; fig. 12f–j).

When the response variable was the inside:outside *SSB*' ratio, results were more similar to those for the small home range case: there was high accuracy for all values of survival variability cv_θ and proxy correlation strength ρ (fig. 13a–e), and high precision for low values of cv_θ (fig. 13f–g). However, when recruitment was more variable ($cv_\theta \geq 1$) precision was very low except when an effective proxy ($\rho \geq 0.8$) was used, although this only improved precision over short time scales (fig. 13h–j). This result is a consequence of home range movement tending to equalize biomass inside and outside of the MPA (e.g., fig. 7c–d). As a consequence, it would be difficult to distinguish successful from unsuccessful MPAs over short time scales using the inside:outside ratio unless an effective proxy were employed.

It is important to note that the use of the inside:outside ratio depends on the choice of sample locations. Comparing a location in the center of the MPA to a location far outside of the MPA boundary—as we have done here—will produce the highest contrast. The inside:outside ratio will be closer to zero (i.e., less informative) if either inside or outside observations were made closer to the MPA edge, especially for species with larger home ranges. This effect can be seen in Figure 6, which shows how a large home range produces a larger zone over which high "inside" values transition to low "outside" values; making observations inside this transi-

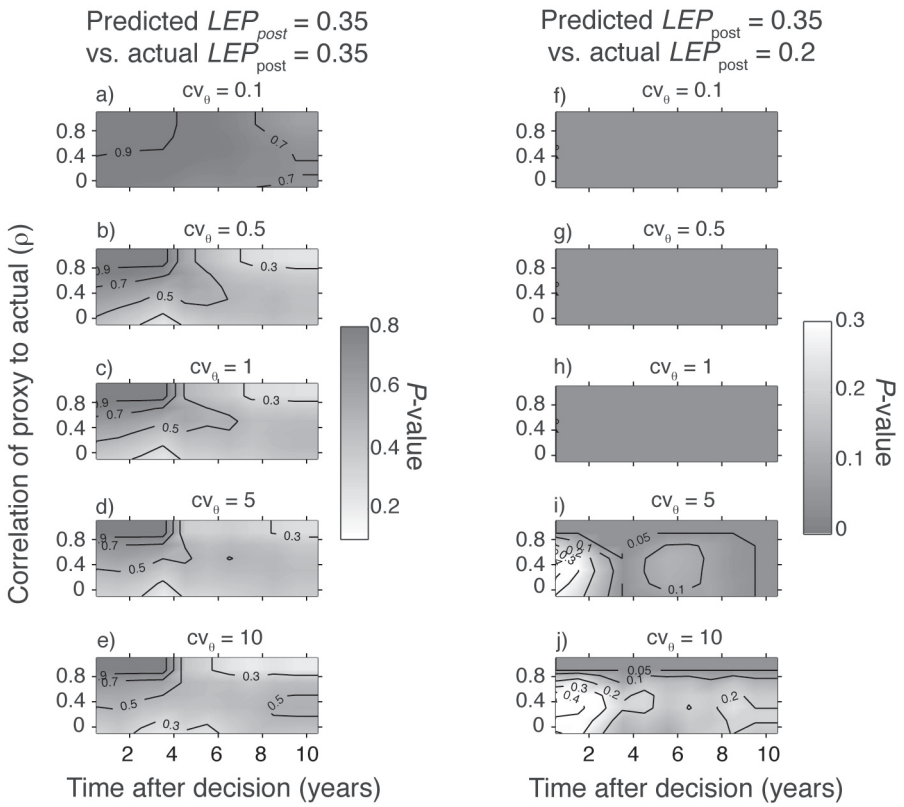

Figure 12. Results from multiple realizations of the spatial model with spatially homogenous dispersal showing the predictive skill of model projections for the ratio of *SSB* after:before MPA implementation. These results were obtained using the forecasting model for a species with long larval dispersal distance (d = 40 km) and large adult home range (h = 10 km); the MPA was 10 km wide. Other figure details as in Figure 10.

tion zone will produce a lower inside:outside ratio. This issue is addressed more formally by Moffitt (2009).

As in the nonspatial case, running the model in hindcast mode improved the accuracy and precision of the model projections, and projections made with a high-ρ proxy were accurate over the entire 10-year period rather than just the initial 4–5 years after the change in fishing pressure (i.e., $t \leq t_c$). For example, in the large-home range (h = 10 km), long larval dispersal (d = 40 km) case, the after:before comparison had greater precision and accuracy, and the latter did not drop off after t = 4 y (this result is not portrayed in the figures). Similarly, the model skill for the inside:outside comparison was high for high values of ρ and cv_θ over the entire 10-year period rather than the first 4 years only.

In these simulations, there was very little effect of the larval retention zone on the efficacy of using the physical proxy, and results were generally similar to those with spatially homogenous dispersal. For comparison, the forecast after:before and inside:outside ratios for the short- and long-home range cases are shown in Figures 14–15. Larval retention can have a striking effect on population persistence within MPAs (White et al. 2010a), and the large home range/short larval dispersal case (h = 10 km, d = 40 km) was persistent with LEP_{post} = 0.2 in the retention zone scenario but not in the homogenous dispersal scenario. Despite the effects on population persistence, the degree of retention that we modeled was not sufficient to substantially alter *SSB*' for the other life history combinations or values of LEP_{post} we considered.

To explore the importance of persistence on the usefulness of the proxy, we also simulated dynamics for a coastline with a much smaller, 3 km wide MPA. This MPA was too small to be self-persistent for any of the larval dispersal distances we considered, although larval production in the fished region was sufficient (under all values of LEP_{post} we considered) for the population to be persistent in all cases except for the long larval dispersal distance and large home range case (d = 40 km, h = 10 km). Despite the lack of self-persistence, results for the small MPA were nearly identical to those for the larger, 10 km MPA. The only noticeable difference was for the inside:outside comparison in the high d, high h scenario, in which the population continued to decline after MPA implementation for all values of LEP_{post}. As a consequence, it was difficult to distinguish alternative LEP_{post} scenarios unless there was very little variability in survival or the proxy correlation strength ρ was very

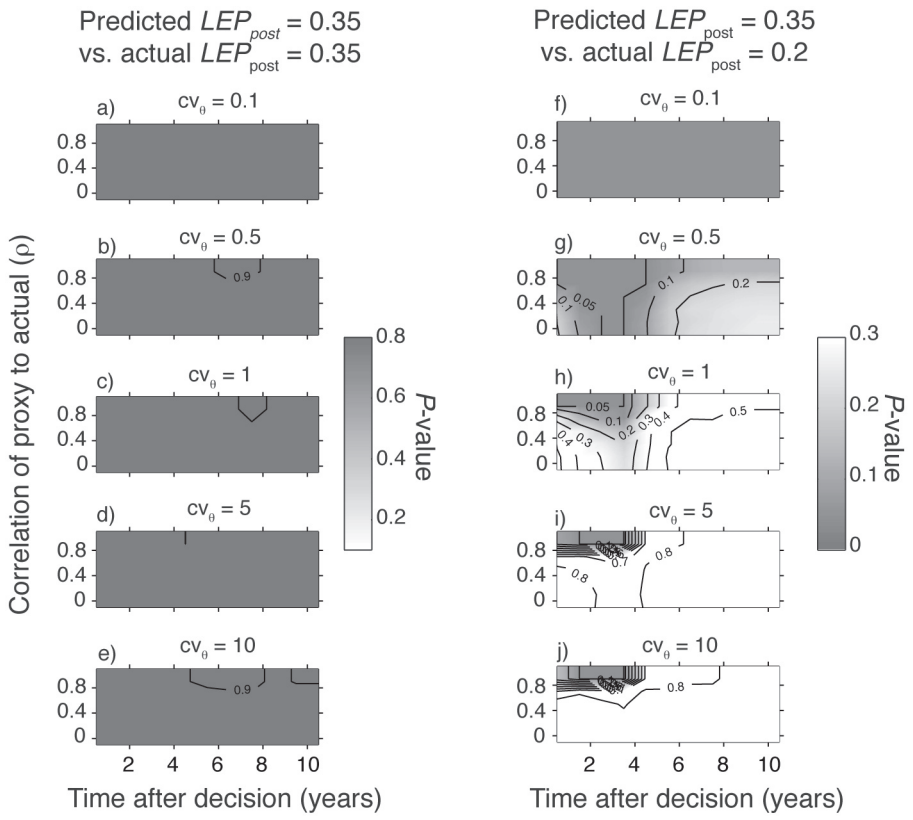

Figure 13. Results from multiple realizations of the spatial model with spatially homogenous dispersal showing the predictive skill of model projections for the ratio of *SSB* inside:outside the MPA. These results were obtained using the forecasting model for a species with long larval dispersal distance (d = 40 km) and large adult home range (h = 10 km); the MPA was 10 km wide. Other figure details as in Figure 10.

high; even with high ρ, the model skill was improved only during years 3–5 following implementation (these results are not portrayed in a figure).

DISCUSSION

Here we have outlined a general framework for incorporating physical proxy information into forecasts of recruitment year-class strength for fishery management. Our modeling results illustrated how variability in larval survival can make it difficult to distinguish the effects of different fishing rates on spawning stock biomass (*SSB*) and population persistence. Our proxy-based method may be useful because it accounts for some of this variability in order to obtain better projections of the response of a fished population to management decisions. These results support the development of good proxies of recruitment strength for fishery management. We anticipate that the application and effectiveness of this modeling approach in a real management scenario will depend on species- and location-specific particulars and as we have shown here will depend on how well the proxy describes recruitment.

Here we have found two consistent outcomes regarding the use of a physical recruitment proxy in forecast models. First, incorporating information from the proxy was most useful when the correlation, ρ, between the proxy and larval survival was high; ≥ 0.8. Correlations this high or higher have been reported for real datasets (e.g., Caselle, this issue; Shanks, this issue), so this approach is promising for implementation. Second, when forecasting for fishery management, the proxy only improves model accuracy out to approximately a_c years, the time to recruitment into the fishery (a time period of 4–5 years in this model). After this point there is a sharp decline in accuracy, because the pre-recruit age classes predicted by the proxy at time t = 0 have entered the fished population, and there is no proxy information on later age classes (i.e. those that were spawned after t = 0). Accuracy falls sharply because the model simulations were no longer tracking the actual population trajectories, despite the well behaved narrow prediction intervals.

Beyond this time ($t > a_c$), the model prediction interval expands, reflecting greater uncertainty about recruitment year class strength, and because the interval is so large it once again tends to encompass the actual value. This anomaly is a feature of the forecast model, but not the hindcast model, for which information on larval survival is available after $t = a_c$ and model accuracy is more

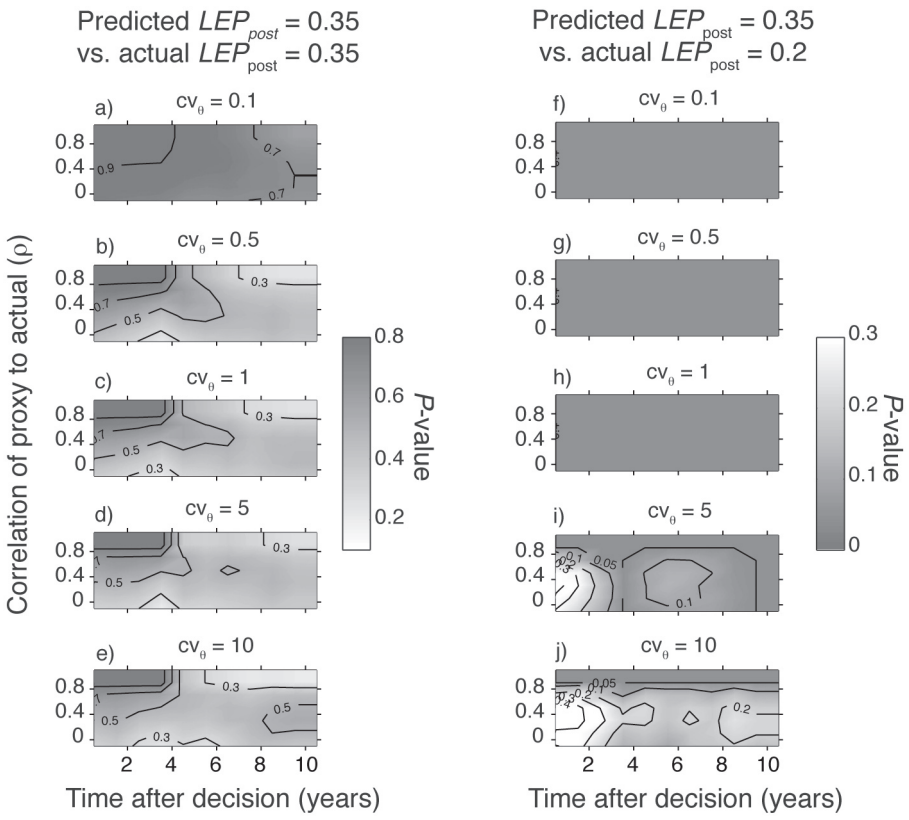

Figure 14. Results from multiple realizations of the spatial model with a larval retention zone showing the predictive skill of model projections for the ratio of SSB after:before MPA implementation. These results were obtained using the forecasting model for a species with long larval dispersal distance (d = 40 km) and large adult home range (h = 10 km); the MPA was 10 km wide. The MPA contains the larval retention zone, inside which larval dispersal distance d is reduced by 50%. Other figure details as in Figure 10.

consistent across time. Thus the use of the proxy is even more advantageous in hindcasting situations over longer periods of time. The time lag in recruitment to the fishery and the width of the prediction interval will be specific to the species examined and the time to enter the fishery. In the example modeled here, kelp rockfish enter the fishery after 4 years, making forecasts beyond this time less reliable. By contrast, a species such as red abalone (*Haliotis rufescens*) enters the fishery in 11 years (Rogers-Bennett et al. 2007), potentially making proxy-derived forecasts reliable over a longer time period.

It is important to note that our models did not account for observation error in the measurement of either physical variables, year class strength, or biomass. It is possible that actual proxies would require a correlation strength considerably better than 0.8 in order to overcome errors introduced by observation and possibly other processes not included in our model.

The use of a recruitment proxy could be especially valuable for short-term decision making with regard to MPAs. There is often little baseline observation data available prior to MPA implementation, especially data that are spatially explicit and collected both inside and outside of MPA sites (e.g., Hamilton et al. 2010). Furthermore, MPAs are politically contentious so there is often a short window for re-evaluation (e.g., 5 yr in California; CDFG 2008) within which recruitment variability could easily overwhelm any signal of an actual deterministic fishing effect within an MPA.

Several authors have recently advocated using inside:outside ratios to avoid the problem of minimal pre-monitoring (E. A. Babcock and A. D. MacCall, unpublished manuscript). Indeed, the inside:outside ratio can be predicted by models relatively well, even without a larval survival proxy, especially in low-variability cases (figs. 11 and 13). However, the use of the inside:outside ratio as a decision rule is predicated on the assumption that biomass inside the MPA is close to the unfished value or differs dramatically with the biomass inside the MPA at the final census period (e.g., 5 years). This will be true only over longer time scales and may not be true for all species (e.g., species with large home ranges; fig. 7c; White et al. 2010b). Additionally, the inside:outside ratios are sensitive to other factors which we did not address in this study, including the distribution of suitable habitat, the spatial distribution of fishing effort, and even the locations at which observations are made. Over short time scales following implementation, or in the case of

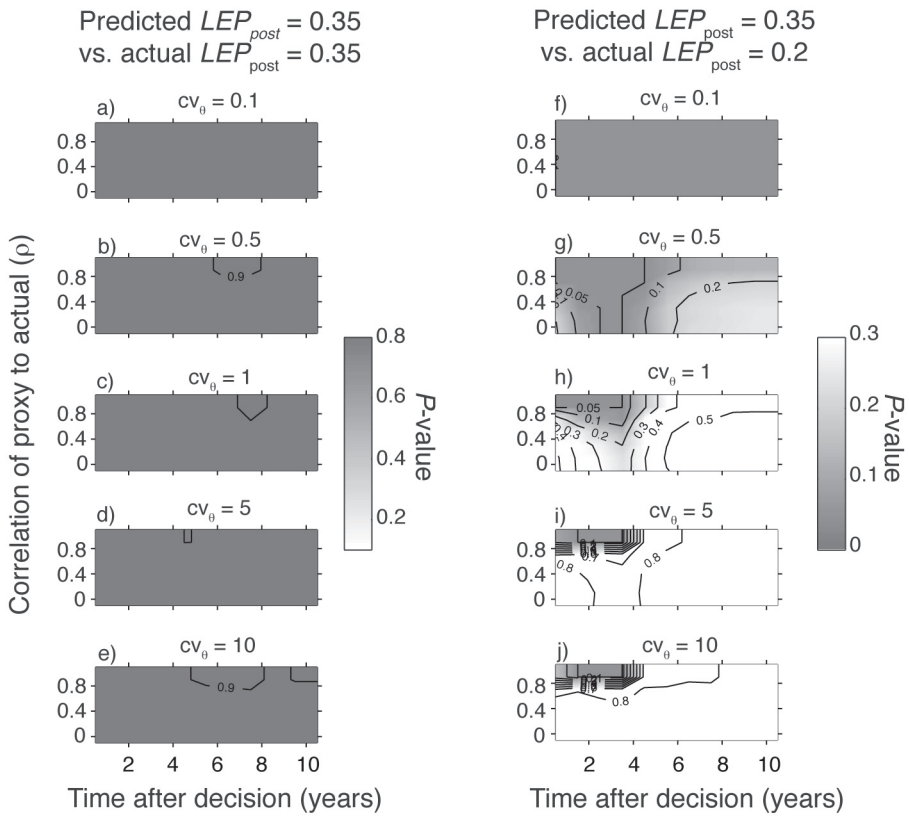

Figure 15. Results from multiple realizations of the spatial model with a larval retention zone showing the predictive skill of model projections for the ratio of SSB inside:outside the MPA. These results were obtained using the forecasting model for a species with long larval dispersal distance (d = 40 km) and large adult home range (h = 10 km); the MPA was 10 km wide. The MPA contains the larval retention zone, inside which larval dispersal distance d is reduced by 50%. Other figure details as in Figure 10.

ineffective MPAs, management strategy evaluations suggest that such ratio-based decision rules may produce unusual and incorrect results (E. A. Babcock and A. D. MacCall, unpublished manuscript). Consequently, we suggest there is value in using our proxy-based method to project results over the short time scales that are most relevant to adaptive management decisions. Ratios obtained from monitoring data could then be evaluated in the context of the expected trajectory of biomass inside and outside the MPAs, reducing the chance that managers draw incorrect inferences from the raw ratios in the absence of proxy information.

Prior modeling efforts have clearly demonstrated that the level of fishing outside MPA boundaries can have an effect on population persistence and biomass inside the MPA (Holland and Brazee 1996; Mangel 1998, 2000; Botsford et al. 2001; White et al. 2010b), just as we found in our spatial model. This result is generally borne out by empirical findings that species targeted by fisheries have a greater response to protection in MPAs (Micheli et al. 2004; Lester et al. 2009; Pelc et al. 2009; Hamilton et al. 2010). As a consequence, the adaptive management of MPAs must utilize model predictions that account for fishing rates outside MPAs. However, while the long-term deterministic trends in biomass associated with different fishing rates tend to be quite distinct (White et al. 2010b), our results show that stochastic variability in larval supply can make it difficult to discern those long-term trends from variability due to recruitment fluctuations over short time scales (e.g., fig. 7d; also see Moffitt 2009). Consequently, the predictions of deterministic models without proxy information should be used with caution in an adaptive management setting.

The Before-After Control-Impact (BACI) approach for detecting management effects is intended to control for the type of stochastic variation modeled here (Underwood 1994). However, our results suggest that the effectiveness of BACI depends on the life history of the species in question. For fishes with small home ranges, the before: after ratio had limited resolution. The prediction intervals of model forecasts for different levels of fishing (LEP_{post}) had considerable overlap, so it would be impossible to distinguish alternative outcomes (e.g., *SSB* might not differ significantly under different management scenarios) in an adaptive management set-

ting. This is an important point for the implementation of this modeling approach. However, an inside:outside comparison was much more accurate and precise in the model forecasts. The opposite was true for species with larger home ranges: there was greater overall effect of LEP_{post} on biomass across the entire coast, so it was easier to resolve different model trajectories using the after:before ratio than using the inside:outside comparison. In general, increasing variability in larval survival impaired the model's prediction of either of these metrics, but substantially improved the model's predictions with the use of an accurate proxy ($\rho > 0.8$). Therefore, we advocate the use of larval survival information in fishery models particularly in cases where research has determined that larval survival is tightly linked to a physical proxy such as an index of upwelling.

A variety of recent spatially explicit modeling efforts have documented the effects of different larval dispersal patterns on MPA performance (McGilliard and Hilborn 2009; Costello et al. 2010; White et al. 2010a), yet we found relatively little effect of larval dispersal distance or larval retention on the accuracy and precision of different effectiveness metrics. In contrast, we did find a large impact of adult home range size on model outcomes, highlighting the importance of basic research describing home ranges of marine organisms. While we did not explore a full suite of larval dispersal distances, we did consider scenarios in which MPAs were large enough relative to the larval dispersal distance to support a self-persistent population as well as scenarios in which this condition was not me. Thus our results do illustrate an insensitivity to larval dispersal over a range of possible population outcomes. A wider range of combinations of MPA size and spacing could be simulated to further investigate this question, but given the potentially large number of parameter combinations involved, we advocate examining real-world scenarios of interest. While little is known about larval dispersal distances, many species with potentially long-distance dispersal (long larval stages) may be retained locally with few individuals dispersing long distances (Strathmann et al. 2002; Marko et al. 2007; Rogers-Bennett and Rogers 2008), so self persistence at the spatial scale of MPAs may be relatively common. In any case, our results suggest that there is not likely to be a strong effect of larval dispersal distance on the effectiveness of management efforts, but there may be an effect adult home ranges sizes.

In summary, our simulations suggested that a physical proxy with a correlation coefficient of greater than 0.8 does function to increase the short-term predictive skill of forecasting and hindcasting models in both the nonspatial and spatial model. In the spatially explicit model (with MPAs) the inclusion of a good physical proxy information improved model precision especially in cases of adults with short home-ranges. Our approach could be applied to adaptive management efforts over short time scales. Numerous authors have documented correlations between physical factors and recruitment year class strength that exceed this level of correlation. Several promising examples emerged from this CalCOFI Symposium, including correlations of up to $r = 0.99$ between annual settlement of KGBC rockfish (primarily kelp rockfish, *Sebastes atrovirens*) and a monthly upwelling index (Caselle et al., this issue), and correlations between Dungeness crab (*Cancer magister*) recruitment and the timing of the spring transition ($r = 0.97$, excluding three recent outlier years) and the Pacific Decadal Oscillation ($r = 0.73$; Shanks et al., this issue). Indices related to upwelling and the Pacific Decadal Oscillation are likely to be informative for many nearshore fisheries on the U.S. Pacific coast, but any number of other environmental indices may be useful for fisheries in other locations (e.g., Vance et al. 1985; Caputi et al. 2001; but see Myers 1998). Short-term predictive powers of these models may improve management performance more for extremely productive populations as opposed to less productive stocks (Walters 1989) and be more beneficial for populations with wide rather than narrow population fluctuations between years. It is precisely these types of fisheries that are challenging to manage. It seems obvious that ocean conditions have a large impact on recruitment and yet traditional fishery management does not incorporate this information into management. In the United States, federal managers have called for the incorporation of physical parameters into models for adaptive management (e.g., the Fisheries And The Environment [FATE] program; http://fate.nmfs.noaa.gov/) and the framework provided here helps to address this goal. This work provides a first step towards incorporating proxies of productivity driven by environmental forcing into modeling to improve fishery management.

ACKNOWLEDGEMENTS

We would like to thank fellow members of the 2009 CalCOFI symposium on forecasting for their presentations and helpful discussions on forecasting productivity and fishery management. L. Rogers-Bennett was supported by the California Department of Fish and Game. J. W. White was supported by grants to L. W. Botsford from the Resource Legacy Fund Foundation, California SeaGrant, and NSF GLOBEC. This is a contribution of the UC Davis Bodega Marine Laboratory.

LITERATURE CITED

A'mar, Z. T., A. E. Punt, and M. W. Dorn. 2008. The management strategy evaluation approach and the fishery for walleye pollock in the Gulf of Alaska. Alaska Sea Grant College Program AK-SG-08-01: 317–346.

Botsford, L. W., and D. E. Wickham. 1974. Correlation of upwelling index and Dungeness crab catch. Fish. Bull. 73: 901–907.

Botsford, L. W., C. L. Moloney, A. Hastings, J. L. Largier, T. M. Powell, K. Higgins, and J. F. Quinn. 1994. The influence of spatially and temporally varying oceanographic conditions on meroplanktonic metapopulations. Deep-Sea Res. II 41: 107–145.

Botsford, L. W., A. Hastings, and S. D. Gaines. 2001. Dependence of sustainability on the configuration of marine reserves and larval dispersal distance. Ecol. Lett. 4: 144–150.

California Department of Fish and Game (CDFG). 2008. California Marine Life Protection Act master plan for marine protected areas. http://www.dfg.ca.gov/mlpa/masterplan.asp. Accessed 4/4/2008.

Caputi, N., C.F. Chubb, and A. Pearce. 2001. Environmental effects on recruitment of the western rock lobster, *Panulirus cygnus*. Mar. Freshw. Res. 52: 1167–1175.

Caselle, J. E., B. P. Kinlan, and R. R. Warner. 2010. Temporal and spatial scales of influence on near-shore fish settlement in the Southern California Bight. Bull. Mar. Sci. 86: 355–385.

Caselle, J. E., B. P. Kinlan, R. R. Warner, D. Malone, and M. H. Carr. In press. Predictability of settlement of nearshore rockfishes (genus *Sebastes*) using simple indices of ocean conditions. Calif. Coop. Oceanic Fish. Invest. Rep.

Costello, C., A. Rassweiler, D. Siegel, G. De Leo, F. Micheli, and A. Rosenberg. 2010. The value of spatial information in MPA network design. Proc. Natl. Acad. Sci. USA. DOI: 10.1073/pnas.0908057107.

Cushing, D. H. 1982. Climate and fisheries. Academic Press, London.

Drechsler, M., and M. A. Burgman. 2004. Combining population viability analysis with decision analysis. Biodiv. Cons. 13: 115–139.

Fogarty, M. J., M. P. Sissenwine, and E. B. Cohen. 1991. Recruitment variability and the dynamics of exploited marine populations. Trends Ecol. Evol. 6: 241–246.

Fraschetti, S., A. Terlizzi, F. Micheli, L. Benedetti-Cecchi, and F. Boero. 2002. Marine protected areas in the Mediterranean Sea: objectives, effectiveness and monitoring. Mar. Ecol. 23 (s1): 190–200.

Freiwald, J. 2009. Causes and consequences of the movement of temperate reef fishes. Ph.D. dissertation. University of California, Santa Cruz, CA, USA.

Gaines, S. G., and M. Bertness. 1993. The dynamics of juvenile dispersal: why field ecologists must integrate. Ecology 74: 2430–2435.

Grafton, R. Q., and T. Kompas. 2005. Uncertainty and the active adaptive management of marine reserves. Mar. Pol. 29: 471–479.

Halpern, B. S., and R. R. Warner. 2003. Matching marine reserve design to reserve objectives. Proc. R. Soc. Lond. B 270: 1871–1878.

Hamilton, S. L., J. E. Caselle, D. P. Malone, and M. H. Carr. 2010. Incorporating biogeography into evaluations of the Channel Islands marine reserve network. Proc. Natl. Acad. Sci. USA. DOI: 10.1073/pnas.0908091107.

Harwood, J., and K. Stokes. 2003. Coping with uncertainty in ecological advice: lessons from fisheries. Trends Ecol. Evol. 18: 617–622.

Hastings, A., and L. W. Botsford. 2006. Persistence of spatial populations depends on returning home. Proc. Natl. Acad. Sci. USA 103: 6067–6072.

Hilborn, R., and M. Mangel. 1997. The ecological detective: confronting models with data. Princeton University Press, Princeton, NJ.

Hilborn, R., A. Parma, and M. Maunder. 2002. Exploitation rate reference points for west coast rockfish: are they robust and are there better alternatives? N. Amer. J. Fish. Manag. 22: 365–375.

Hill, K. T., E. Dorval, N. C. H. Lo, B. J. Macewicz, C. Show, R. Felix-Uraga. 2007. Assessment of the Pacific sardine resources in 2007 for U. S. management in 2008. NOAA Technical Memorandum NMFS-SWFSC-413.

Hjort, J. 1914. Fluctuations in the great fisheries of northern Europe. Rapp. P.-V. Reun. Cons. Inst. Explor. Mer. 20: 1–13.

Holland, D. S., and R. J. Brazee. 1996. Marine reserves for fisheries management. Marine Resource Economics 11: 157–171.

Lea, R. N., R. D. McAllister, and D. A. VenTresca. 1999. Biological aspects of nearshore rockfishes of the genus *Sebastes* from Central California with notes on ecologically related sport fishes. California Dept. Fish and Game Fish Bull. 177.

Lester, S. E., B. S. Halpern, K. Grorud-Colvert, J. Lubchenco, B. I. Ruttenberg, S. D. Gaines, S. Airamé, and R. R. Warner. 2009. Biological effects within no-take marine reserves: a global synthesis. Mar. Ecol. Prog. Ser. 384: 33–46.

Love M. S., M. M. Yoklavich, and L. Thorsteinson. 2002. The rockfishes of the northeast Pacific. Berkeley, California: University of California Press. 404 pp.

Mangel, M. 1998. No-take areas for sustainability of harvested species and a conservation invariant for marine reserves Ecol. Lett. 1: 87–90.

Marko, P. B., L. Rogers-Bennett, and A. B. Dennis. 2007. MtDNA population structure and gene flow in lingcod (*Ophiodon elongatus*): limited connectivity despite long-lived pelagic larvae. Mar. Biol. 150: 1301-1311.

McClatchie, S., R. Goericke, G. Auad, and K. Hill. 2010. Re-assessing the temperature index for Pacific sardine (*Sardinops sagax*) stock assessment. Can. J. Fish. Aquat. Sci.

McGilliard, C. R., and R. Hilborn. 2009. Modeling no-take marine reserves in regulated fisheries: assessing the role of larval dispersal. Can. J. Fish. Aquat. Sci. 65: 2509–2523.

Micheli, F., B. S. Halpern, L. W. Botsford, and R. R. Warner. 2004. Trajectories and correlates of community change in no-take marine reserves. Ecol. Appl. 14: 1709–1723.

Moffitt, E. A. 2009. The design and implications of marine protected areas for mobile species: a theoretical approach. Ph.D. dissertation, University of California, Davis, CA, USA.

Moffitt, E. A., L. W. Botsford, D. M. Kaplan, and M. R. O'Farrell. 2009. Marine reserve networks for species that move within a home range. Ecol. Appl. 19: 1835–1847.

Mullin, M. M. 1994. Webs and scales: Physical and ecological processes in marine fish recruitment. Washington Sea Grant Program/University of Washington Press, Seattle and London.

Myers, R. A. 1998. When do environment-recruitment correlations work? Rev. Fish. Biol. Fish. 8: 285–305.

O'Farrell, M. R., and L. W. Botsford. 2005. Estimation of change in lifetime egg production from length frequency data. Can. J. Fish. Aquat. Sci. 62: 1626–1639.

Pelc, R. A., M. L. Baskett, T. Tanci, S. D. Gaines, and R. R. Warner. 2009. Quantifying larval export from South African marine reserves. Mar. Ecol. Prog. Ser. 394: 65–78.

Peterman, R. M., and J. R. Anderson. 1999. Decision analysis: a method for taking uncertainties into account in risk-based decision making. Hum. Ecol. Risk. Assess. Int. J. 5: 231–244.

Peterson, W. T., and F. B. Schwing. 2003. A new climate regime in northeast Pacific ecosystems. Geophys. Res. Lett. 30: 1896.

Punt, A., and S. Ralston. 2007. A management strategy evaluation of rebuilding revision rules for overfished rockfish stocks. Alaska Sea Grant College Program AK-SG-07-01: 329–351.

Punt, A. E., A. D. M. Smith, and G. Cui. 2002. Evalution of management tools for Australia's South East Fishery 1. modelling the South East Fishery taking account of technical interactions. Mar. Freshw. Res. 53: 615–629.

Ralston, S. 2002. West coast groundfish harvest policy. N. Amer. J. Fish. Manag. 22: 249-250.

Roberts, C. M., S. Andelman, G. Branch, R. H. Bustamante, J. C. Castilla, J. Dugan, B. S. Halpern, K. D. Lafferty, H. Leslie, J. Lubchenco, D. McArdle, H. P. Possingham, M. Ruckelshaus, and R. R. Warner. 2003. Ecological criteria for evaluating candidate sites for marine reserves. Ecol. Appl. 13: S199–S214.

Rogers-Bennett, L., D. W. Rogers, and S. Schultz. 2007. Modeling growth and mortality of red abalone (*Haliotis rufescens*) in northern California. J. Shellfish Res. 26: 719–727.

Rogers-Bennett, L., and D.W. Rogers 2008. Modeling dispersal of cloning echinoderm larvae with a Gaussian distribution: Forever young? CalCOFI Reports 49: 232–240.

Rose, K. A., and J. H. Cowan, Jr. 2003. Data, models, and decisions in U.S. marine fisheries management: lessons for ecologists. Ann. Rev. Ecol. Syst. 34: 127–151.

Russ, G. R., A. J. Cheal, A. M. Dolman, M. J. Emslie, R. D. Evans, I. Miller, H. Sweatman, and D. H. Williamson. 2008. Rapid increase in fish numbers follows creation of world's largest marine reserve network. Curr. Biol. 18: R514–R515.

Shanks, A., G. C. Roegner, and J. Miller. In press. Predicting the future commercial catch of Dungeness crabs. Calif. Coop. Oceanic Fish. Invest. Rep.

Shepherd, J. G., and D. H. Cushing. 1990. Regulation in fish populations: myth or mirage? Phil. Trans. R. Soc. Lond. B. 330: 151–164.

Strathmann, R. R., T. P. Hughes, A. M. Kuris, K. C. Lindeman, S. G. Morgan, J. M. Pandolfi, and R. R. Warner. 2002. Evolution of local recruitment and its consequences for marine populations. Bull. Mar. Sci. 70 (Suppl): 377–396.

Underwood, A. J. 1994. On beyond BACI: sampling designs that might reliably detect environmental disturbances. Ecol. Appl. 4: 3–15.

Vance, D. J., D. J. Staples, and J. D. Kerr, 1985. Factors affecting year-to-year variation in the catch of banana prawns *Penaeus merguiensis* in the Gulf of Carpentaria, Australia. J. Cons. Int. Explor. Mer 42: 83–97.

Walters, C. J. 1989. Value of short-term forecasts of recruitment variation for harvest management. Can. J. Fish. Aquat. Sci. 46: 1969–1976.

Walters, C. J. 1997. Challenges in adaptive management of riparian and coastal ecosystems. Cons. Ecol. 1: 1.

White, J.W. 2010. Adapting the steepness parameter from stock-recruit curves for use in spatially explicit models. Fish. Res. 102: 330–334.

White, J.W., L.W. Botsford, A. Hastings, and J.L. Largier. 2010a. Population persistence in marine reserve networks: incorporating spatial heterogeneities in larval dispersal. Mar. Ecol. Prog. Ser. 398: 49-67.

White, J. W., L. W. Botsford, E. A. Moffitt, and D. T. Fischer. 2010b. Decision analysis for designing marine protected areas for multiple species with uncertain fishery status. Ecological Applications 20: 1523–1541.